Underwater Sound Associated with the Tilt Cove Exploration Drilling Project

Jeanne d'Arc Basin, Offshore Eastern Newfoundland

Submitted to:
Ellen Tracy
Stantec Consulting Ltd.
Job Number: 121416216

Authors:
Zahra Alavizadeh
Terry J. Deveau

16 January 2020

P001498-001
Document 01845
Version 1.0

JASCO Applied Sciences (Canada) Ltd.
202–32 Troop Avenue
Dartmouth, NS B3B 1Z1 Canada
Tel: +1-902-405-3336
Fax: +1-902-405-3337
www.jasco.com

Document Version Control

Version	Date	Name	Change
1.0	16 Jan 2020	Terry J. Deveau	Final version for release.

Suggested citation
Alavizadeh, Z, and T.J. Deveau. 2020. *Underwater Sound Associated with the Tilt Cove Exploration Drilling Project: Jeanne d'Arc Basin, Offshore Eastern Newfoundland*. Document 01845, Version 1.0. Technical report by JASCO Applied Sciences for Stantec Consulting Ltd.

Disclaimer:

The results presented herein are relevant within the specific context described in this report. They could be misinterpreted if not considered in the light of all the information contained in this report. Accordingly, if information from this report is used in documents released to the public or to regulatory bodies, such documents must clearly cite the original report, which shall be made readily available to the recipients in integral and unedited form.

Contents

Figures

Tables

1. Introduction

JASCO Applied Sciences (JASCO) undertook an acoustic propagation modelling study for Stantec Consulting Ltd. (Stantec) to predict underwater sound levels associated with the proposed Tilt Cove exploration drilling project. The exploration drilling program is proposed by Suncor Energy Offshore Exploration Partnership (Suncor) to operate on exploration license block EL-1161. The EL-1161 block is located off eastern Newfoundland in the Jeanne d'Arc Basin (Figures 1 and 2).

The exploration program will require drilling and Vertical Seismic Profiling (VSP) to be performed. The project may involve drilling up to 12 wells over the 2019 to 2028 time period. These activities will introduce underwater sound into the environment, which could potentially adversely impact marine mammals and fish. At the time of this modelling study, the exact equipment for the proposed project had not been finalized. JASCO identified equipment models that are representative of those commonly used for such activities.

The following operations and associated sound sources were modelled:

- Vertical Seismic Profiling (VSP): seismic airgun array
- Semi-submersible exploratory drilling platform—anchored but with dynamic positioning (DP) thruster assist (this is referenced as the MODU, mobile offshore drilling unit).
- Support/supply vessel.

The goal of the modelling study was to estimate the root-mean-square (rms) pressure level, referred to as sound pressure level (SPL) and the sound exposure level over a 24 h period (SEL_{24h}) for the three representative sources that pertain to the exploratory drilling operations, and the peak sound pressure level (PK) for the seismic source only. A cumulative soundscape study was also performed to consider the total sound field in the project area with sound from the proposed Suncor project added to the sound levels propagating four other production platforms (Hibernia, Hebron, Terra Nova, and White Rose) and drilling at the Hibernia Southern Extension (HSE).

The acoustic characteristics of the airgun array used for the seismic survey were modelled with JASCO's Airgun Array Source Model (AASM, Section 2.1), which accounts for individual airgun volumes and the array geometry. The source levels of the MODU and supply vessel were estimated based on the field measurements of representative examples.

The acoustic propagation modelling for the purpose of assessing the SEL_{24h} field was conducted with JASCO's Marine Operations Noise Model (MONM, Section 2.2.1) for the ranges up to 100 km from the sound sources in the 10 to 25,000 Hz frequency range. Sound propagation modelling for the purpose of calculating peak pressure level (PK) was conducted using a full waveform modelling approach up to 20 km from the acoustic source in the 9 to 891 Hz frequency band.

The acoustic field was modelled at one site within block EL-1161. The modelling was performed for two sound speed profiles in the water column that are historically typical for the two months February and August (Section 3.1), which represent respectively the best and worst seasonal acoustic propagation environments. The Dual Delta 1200 in^3 airgun array was used as a representative example of seismic source for VSP operations. The *Seadrill West Sirius* semi-submersible platform was used an example MODU.

The SEL_{24h} and PK were assessed against the threshold levels for the onset of Permanent Threshold Shift (PTS) relevant to marine mammal groups using respective marine mammal auditory weighting functions (M-weighting functions) as per National Marine Fisheries Service (NMFS 2018) for marine mammals. The (Popper et al. 2019) thresholds were used for assessing impacts on fish.

Section 2 details the methodology for predicting the source levels (Section 2.1) and modelling the sound propagation (Section 2.2). Section 3 describes the input parameters for the propagation modelling: the assumed environmental parameters (Section 3.1), receiver geometry (Section 3.2), and the specifications and derived source levels of the acoustic sources (Section 3.3). Section 4 presents results as sound field

contour maps and tables of ranges to PTS-onset threshold levels. Appendix A explains the metrics used to represent underwater acoustic fields, and Appendix B presents the impact criteria considered.

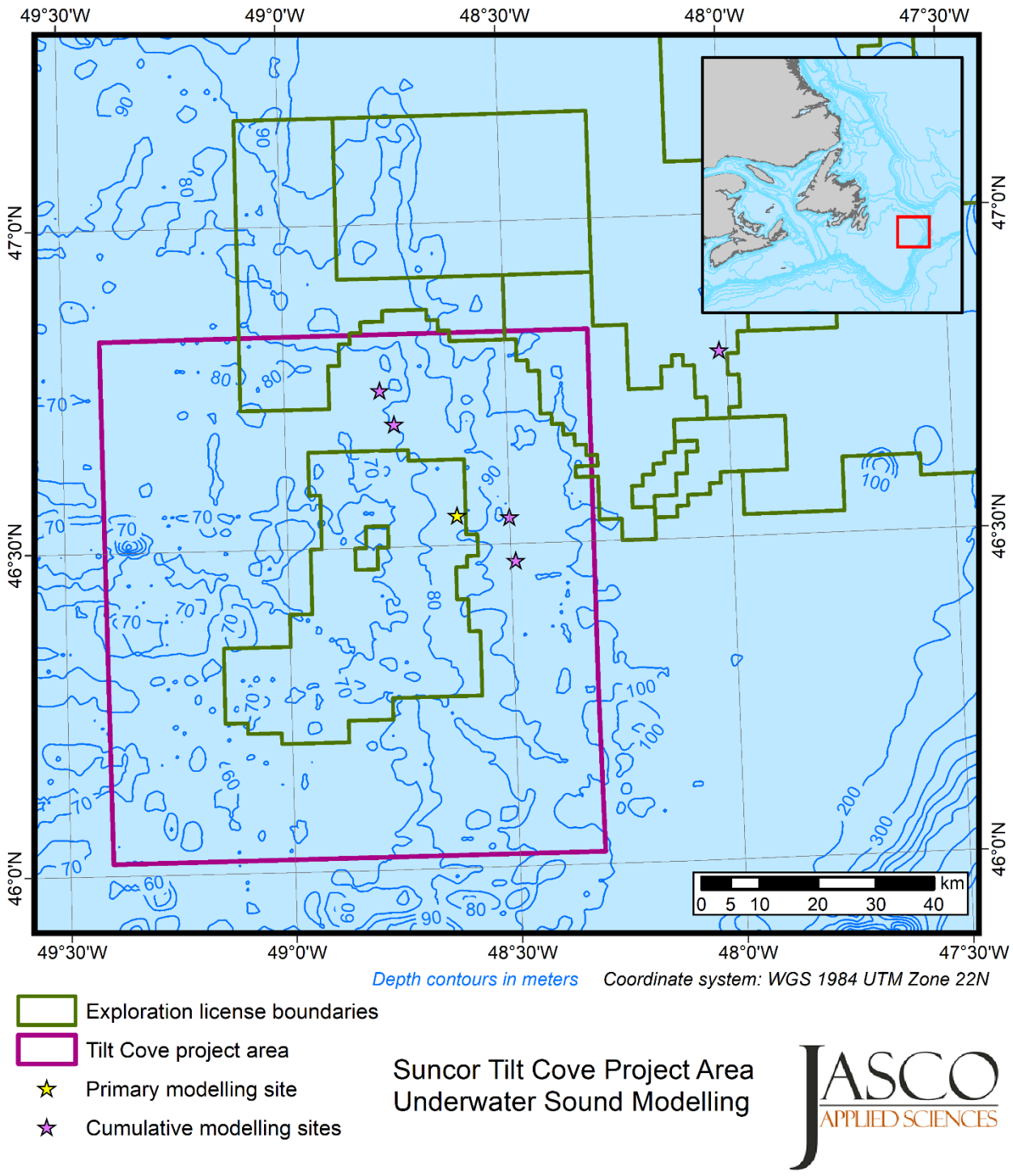

Figure 1. Project area overview and modelled location (stars

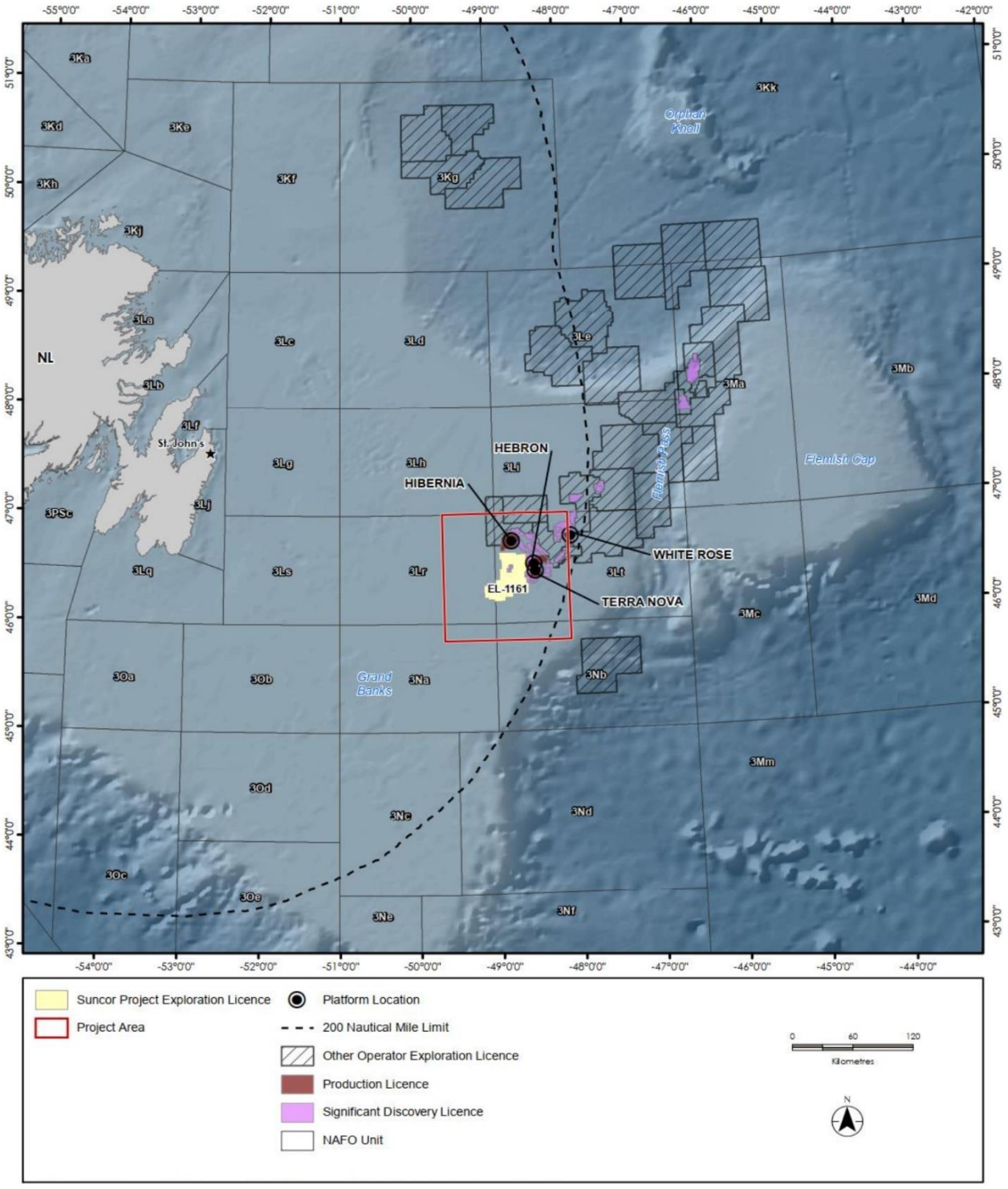

Figure 2. Overview of Suncor project area in relation to other offshore Newfoundland oil and gas projects in the vicinity.

2. Methods

The underwater acoustic fields were predicted by first modelling the source level function and then modelling the pressure wave propagation around the source.

JASCO employed several acoustic source function models and acoustic wave propagation models. The models were selected based on the characteristics of the sound sources and the required output. The models incorporated parameters specific to the modelled source and the environment.

2.1. Acoustic Source Models

2.1.1. Seismic Source

The energy source levels and directivity of the airgun array were predicted with JASCO's Airgun Array Source Model (AASM). This model is based on the physics of the oscillation and radiation of airgun bubbles as described by Ziolkowski (1970). The model solves the set of parallel differential equations that govern bubble oscillations. AASM also accounts for non-linear pressure interactions between airguns, port throttling, bubble damping, and Generated Injection (GI) airgun behavior, as discussed by Dragoset (1984), Laws et al. (1990), and Landro (1992). AASM includes four empirical parameters that are tuned so that the model output matches observed airgun behavior. The model parameters were fit to a large library of empirical airgun data using a "simulated annealing" global optimization algorithm (Černý 1985). These airgun data consist of measured signatures of Bolt 600/B airguns that range in volume from 5 to 185 in^3; the provided sampling rate of the time series was 50 kHz (Racca and Scrimger 1986).

While airgun signatures are highly repeatable at the low frequencies, which are used for seismic imaging, their sound emissions have a large random component at higher frequencies that cannot be predicted deterministically. Therefore, the high-frequency module of AASM uses a stochastic simulation to predict the sound emissions of individual airguns above 800 Hz, using a multivariate statistical model. This model is based on a statistical analysis of a large library of high quality seismic source signature data obtained from the Joint Industry Program (JIP) on Sound and Marine Life (Mattsson and Jenkerson 2008). The stochastic model uses a Monte-Carlo method to simulate the random component of the high-frequency spectrum of each airgun in an array. The mean high-frequency spectra from the stochastic model augment the low-frequency signatures from the physical model, allowing AASM to predict airgun source levels at frequencies up to 25,000 Hz.

AASM produces a set of notional signatures for each airgun element based on:

- Array spatial layout
- Volume, tow depth, and operating pressure of each airgun
- Interactions between airguns in the array

Notional signatures are the pressure waveforms of the individual airguns at a standard reference distance of 1 m; they account for the interactions between the air bubbles created by adjacent airguns in the array. The signatures are summed with the appropriate phase delays to obtain the far-field source signature of the entire array in the horizontal plane. This far-field[1] array signature is filtered into 1/3-octave passbands to compute the energy source levels of the array as a function of frequency band and azimuthal angle in the horizontal plane (at the source depth). It can then be treated as a point source in the far field.

[1] The far-field is the zone where, to an observer, sound originating from a spatially distributed source appears to radiate from a single point. The distance to the acoustic far field increases with frequency.

A seismic array consists of many sources and the point-source assumption is invalid in the near field where the array elements add incoherently. The maximum extent of the near field of an array (R_{nf}) is:

$$R_{nf} < \frac{l^2}{4\lambda} \quad (1)$$

where λ is the sound wavelength and l is the longest dimension of the array (Lurton 2002, §5.2.4). For example, an airgun array length of $l \approx 16$ m yields a near-field range of 85 m at 2 kHz and 17 m at 100 Hz. Beyond R_{nf}, it is assumed that an array radiates like a directional point source and is treated as such for propagation modeling.

The AASM accurately predicts the energy source level of each complete array as a point source for the purpose of acoustic propagation modeling in the far-field; however, predicted energy source levels for 0 to PK and SEL metrics could be higher than the possible maximum levels during the array operation even within the array. AASM accounts for the effects of source depth on bubble interactions, the surface-reflected signal (i.e., surface ghost) is excluded from the far-field source signatures. The propagation models account for surface reflections, a property of the medium rather than the source.

The separations between individual elements of the array in the horizontal plain create directionality in overall acoustic emissions. Generally, this directivity is prominent mainly at frequencies in the mid-range of several tens to several hundreds of hertz; at lower frequencies, where acoustic wavelengths are much larger than the inter-airgun separation distances, directivity is small. At higher frequencies the pattern of lobes becomes too finely spaced to be resolved and the effective directivity is less.

The AASM model can predict the far-field airgun array signature in the frequency range from 10 to 25,000 Hz.

2.1.2. Vessel and MODU Thrusters

Underwater sound that radiates from vessels is produced mainly by propeller and thruster cavitation, with a smaller fraction of sound produced by sound transmitted through the hull, such as by engines, gearing, and other mechanical systems. Sound levels tend to be the highest when thrusters are used to position the vessel and when the vessel is transiting at high speeds. A vessel's sound signature depends on the vessel's size, power output, propulsion system, and the design characteristics of the given system (e.g., blade shape and size). A vessel produces broadband acoustic energy with most of the energy emitted below a few kilohertz. Sound from onboard machinery, particularly sound below 200 Hz, dominates the sound spectrum before cavitation begins—normally around 8–12 knots on many commercial vessels (Spence et al. 2007). Under higher speeds and higher propulsion system loads, the acoustic output from the cavitation processes on the propeller blades dominates other sources of sound on the vessel (Leggat et al. 1981) in the broadband. However, with introduction of the criteria that rely on weighted spectrum it is important to account for the acoustic energy at higher frequencies.

Another common approach for defining the source levels for vessels is to use field measurements from a similar vessel of the same type (a "surrogate" vessel) while involved in a similar activity. The measured relative spectrum levels are taken unchanged, while the broadband level is adjusted to account for any difference in the total propulsion power between the surrogate vessel and the vessel of interest.

This modelling study applied a hybrid method of vessel source level estimation that involves calculation of the sound levels from the cavitating propeller and estimations based on the surrogate vessel approach. The resultant source level spectrum for the support vessel that was used in this study was the calculated spectrum shape from the cavitating propeller scaled in intensity to match the measured broadband level of the surrogate vessel.

2.1.2.1. Sound levels from cavitating propeller

The sound power from the propellers is proportional to the number of blades, the propeller diameter, and the propeller tip speed (Leggat et al. 1981). Based on an analysis of acoustic data, Ross (1976) provided the following formula for the sound levels from a vessel's propeller, operating in calm, open ocean conditions:

$$L_{100} = 155 + 60\log_{10}(u/25) + 10\log_{10}(B/4)\,, \tag{2}$$

where L_{100} is the spectrum level at 100 Hz, u is the propeller tip speed (m/s), and B is the number of propeller blades. Equation 2 gives the total energy produced by the propeller cavitation at frequencies between 100 Hz and 10 kHz. This equation is valid for a propeller tip speed between 15 and 50 m/s. The spectrum is assumed to be flat below 100 Hz. Its level is assumed to fall off at a rate of −6 dB per octave above 100 Hz (Figure 3).

Another method of predicting the source level of a propeller was suggested by Brown (1977). For propellers operating in heavily loaded conditions, the formula for the sound spectrum level is:

$$\mathrm{SL}_B = 163 + 40\log_{10} D + 30\log_{10} N + 10\log_{10} B - 20\log_{10} f + 10\log_{10}(A_c/A_D)\,, \tag{3}$$

where D is the propeller diameter (m), N is the propeller revolution rate per second, B is the number of propeller blades, A_C is the area of the blades covered by cavitation, and A_D is the total propeller disc area. Similar to Ross's approach, the spectrum below 100 Hz is assumed to be flat. Tests with a naval propeller operating at off-design heavily loaded conditions showed that Equation 3 should be used with a value of $\mathrm{A_C}/\mathrm{A_D} = 1$ (Leggat et al. 1981).

If a vessel is equipped with multiple thrusters, the combined source level for a group of thrusters operating together can be estimated using the formula:

$$\mathrm{SL}_{\mathrm{total}} = 10\log_{10}\textstyle\sum_i 10^{\mathrm{SL}_i/10}\,, \tag{4}$$

where $\mathrm{SL}_{1,\ldots,N}$ are the source levels of individual thrusters. If a vessel is equipped with all the same type of thrusters (the source levels are equal), the combined source level can be estimated using the formula:

$$\mathrm{SL}_N = \mathrm{SL} + 10\log_{10} N\,, \tag{5}$$

where N is the total number of thrusters of the same type.

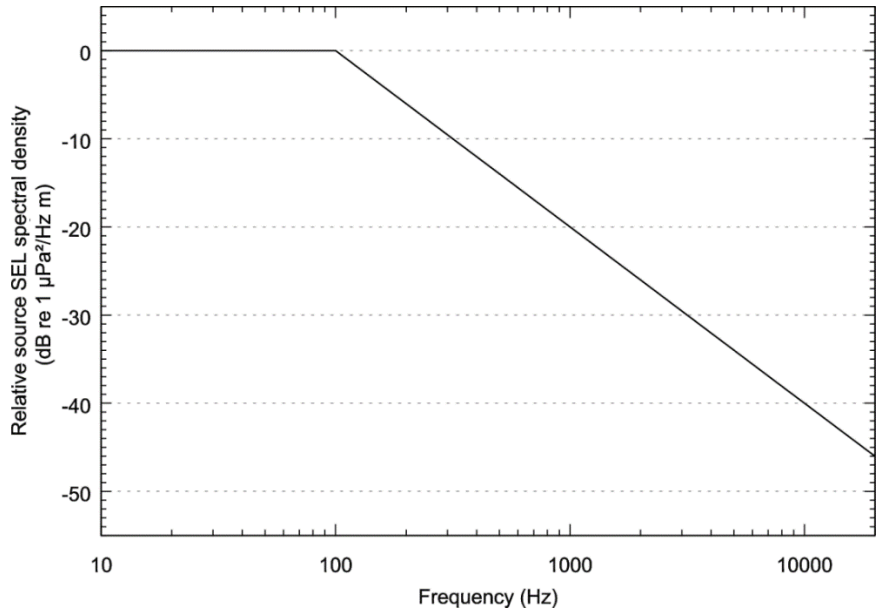

Figure 3. Estimated relative sound spectrum from a cavitating propeller (Leggat et al. 1981).

2.1.2.2. Estimating source levels using the "surrogate" vessel approach

The second common approach for defining the source levels for vessels is to use field measurements completed on a similar vessel of the same type ("surrogate" vessel) involved in a similar activity. The measured spectrum is taken unchanged while the broadband source level is adjusted to account for any difference in the total propulsion power between the reference vessel and the vessel of interest. The adjusted broadband source level is calculated as:

$$SL = SL_{ref} + 10\log_{10}\left({}^{P}/_{P_{ref}}\right), \tag{6}$$

where SL_{ref} is the broadband source level of the surrogate vessel, and P and P_{ref} are the total propulsion power of the vessel of interest and the surrogate vessel, respectively. The relative source level spectrum of the surrogate vessel is left unchanged.

2.2. Sound Propagation Modelling

The sound field around a source can be estimated using two approaches: modelling in bands (usually in decidecade bands) and full waveform modelling. In the decidecade band modelling approach, the sound propagation modelling is performed only for the central frequencies of each band. Only 35 individual frequency modelling runs are required for covering the frequency range from 10 Hz to 25 kHz. For the full waveform approach, the propagation modelling has to be performed for individual frequencies with a constant step across the entire modelled frequency range.

The modelling in bands approach is suitable for efficiently modelling a wide frequency range of the SPL field from continuous sound sources and SEL field from both continuous and impulsive sources.

The full waveform approach, which is much more computationally intensive, outputs a synthetic pressure time domain series that allows direct calculation of metrics such as the SPL and PK levels for impulsive sources.

2.2.1. Energy Propagation Loss Modelling using the Decidecade band Approach

The distribution of a sound's power with frequency is described by the sound's spectrum. The sound spectrum can be split into a series of adjacent frequency bands. Splitting a spectrum into 1 Hz wide bands, called passbands, yields the power spectral density of the sound. This splitting of the spectrum into passbands of a constant width of 1 Hz, however, does not represent how animals perceive sound.

Because animals perceive exponential increases in frequency rather than linear increases, analyzing a sound spectrum with passbands that increase exponentially in size better approximates real-world scenarios. In underwater acoustics, a spectrum is commonly split into decidecade bands, which are approximately one-third of an octave (base 2) wide and often referred as 1/3-octave-bands. Each octave represents a doubling in sound frequency. The centre frequency of the ith band, $f_c(i)$, is defined as:

$$f_{\mathrm{c}}(i) = 10^{\frac{i}{10}} \tag{7}$$

and the low (f_{lo}) and high (f_{hi}) frequency limits of the ith band are defined as:

$$f_{\mathrm{lo},i} = 10^{\frac{-1}{20}} f_{\mathrm{c}}(i) \quad \text{and} \quad f_{\mathrm{hi},i} = 10^{\frac{1}{20}} f_{\mathrm{c}}(i) \tag{8}$$

The decidecade bands become wider with increasing frequency, and on a logarithmic scale the bands appear equally spaced (Figure 4).

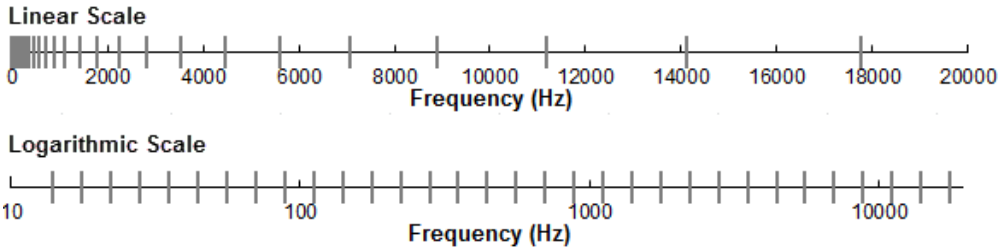

Figure 4. Decidecade frequency bands (vertical lines) shown on a linear frequency scale and a logarithmic scale.

2.2.1.1. Propagation loss modelling

The propagation of sound through the environment can be modeled by predicting the acoustic propagation loss—a measure, in decibels, of the decrease in sound level between a source and a receiver some distance away. Geometric spreading of acoustic waves is the predominant way by which propagation loss occurs. Propagation loss also happens when the sound is absorbed and scattered by the seawater, and absorbed scattered, and reflected at the water surface and within the seabed. Propagation loss depends on the acoustic properties of the ocean and seabed; its value changes with frequency.

If the acoustic energy source level ($L_{S,E}$), expressed in dB re 1 µPa²m²s, and energy propagation loss ($N_{\mathrm{PL},E}$), in units of dB, at a given frequency are known, then the received level ($L_{E,p}$) at a receiver location can be calculated in dB re 1 µPa²s by:

$$L_{E,p}(r) = L_{\mathrm{S},E} - N_{\mathrm{PL},E}(r)\,, \tag{9}$$

where r is the range of the receiver from the source.

JASCO's MONM predicts underwater sound propagation (i.e., propagation loss) at frequencies from 10 to 25,000 Hz. MONM employs two underlying subroutines: MONM-RAM is used for propagating acoustic waves at low frequencies (up to 2000 Hz) and MONM-BELLHOP is used for high frequencies (above 2000 Hz).

MONM-RAM computes acoustic propagation via a wide-angle parabolic equation solution to the acoustic wave equation (Collins 1993) based on a version of the U.S. Naval Research Laboratory's Range-dependent Acoustic Model (RAM), which has been modified to account for an elastic seabed (Zhang and Tindle 1995). The parabolic equation method has been extensively benchmarked and is widely employed in the underwater acoustics community (Collins et al. 1996). MONM-RAM accounts for the additional reflection loss at the seabed due to partial conversion of incident compressional waves to shear waves at the seabed and sub-bottom interfaces, and it includes wave attenuations in all layers. MONM-RAM incorporates the following site-specific environmental properties: a modeled area bathymetric grid, underwater sound speed as a function of depth, and a geoacoustic profile based on the overall stratified composition of the seafloor.

MONM-BELLHOP employs Gaussian beam acoustic ray-trace model (Porter and Liu 1994). This version of MONM accounts for sound attenuation due to energy absorption through ion relaxation and viscosity of water in addition to acoustic attenuation due to reflection at the medium boundaries and internal layers (Fisher and Simmons 1977). The former type of sound attenuation is significant for frequencies higher than 5 kHz and cannot be neglected without noticeably affecting the model results. MONM-BELLHOP incorporates the following site-specific environmental properties: a modeled area bathymetric grid, underwater sound speed as a function of depth, average temperature and salinity in the water column for calculating the sound attenuation due to energy absorption, and geoacoustic properties of the surficial sediments.

The accuracy of MONM's predictions have been validated against experimental data from several sound source verification programs conducted by JASCO (Hannay and Racca 2005, Aerts et al. 2008, Funk et al. 2008, Ireland et al. 2009, O'Neill et al. 2010, Warner et al. 2010).

The propagation loss values calculated for each individual band are subject to range averaging that replaces frequency averaging (Harrison and Harrison 1995, Siderius and Porter 2006). The range averaging technique allows us to increase the accuracy with which propagation loss function calculated for single frequency matches the band average propagation loss calculated using 1 Hz step frequency propagation loss functions.

2.2.1.2. Summing over decidecade bands

In case the source emits acoustic energy that spans across multiple frequency bands, the composite broadband received SEL can be computed by summing the received decidecade band levels (provided in dB units):

$$L_E = 10 \log_{10} \left(\sum_{i=1}^{N} 10^{\frac{L_{E,i}}{10}} \right). \quad (10)$$

If frequency weighed SEL is required ($L_{E,\mathrm{MW}}$) for the impact assessment with criteria thresholds (Appendix B), it can be obtained by adding the relative levels (MW) to the equation:

$$L_{E,\mathrm{MW}} = 10 \cdot \log_{10} \sum_{i=1}^{N} 10^{(L_E,i+\mathrm{MW}_i)/10} \ . \quad (11)$$

2.2.2. Full Waveform Modelling

For impulsive sounds, time-domain representations of the pressure waves generated in the water are required for calculating SPL and PK. The synthetic pressure waveforms can be computed using Full Waveform Range-dependent Acoustic Model (FWRAM), which is a time-domain acoustic model based on the same wide-angle parabolic equation (PE) algorithm as MONM-RAM (Section 2.2.1.1). FWRAM computes synthetic pressure waveforms (Figure 5) for virtual receivers placed at various ranges from the source and through the water column. The computations occur for range-varying marine acoustic environments, and it takes the same environmental inputs as MONM-RAM (bathymetry, water sound speed profile, and seabed geoacoustic profile). FWRAM computes pressure waveforms via Fourier synthesis of the modelled acoustic transfer function in closely spaced frequency bands. FWRAM employs the array starter method to further increase accuracy of the sound propagation modeling from a spatially distributed source (MacGillivray and Chapman 2012).The FWRAM modelling method requires propagation modelling to be performed at frequencies with constant step across the entire frequency range of interest. The frequency step (Δf) is defined by the necessary length of the time series (t):

$$\Delta f = {}^{1}/_{t} \, . \quad (12)$$

Therefore, to produce a 2 second long time series, the modelling frequency step needs to be 0.5 Hz, and for 0.5 second long time series–2 Hz step.

Full waveform modelling is substantially more computationaly extensive compared to the propagation loss in bands modelling approach. It is performed within a narower frequency band with practical top limit at 2000 Hz and fewer modelling profiles. Because most acoustic energy emmited by a seismic source is below 500 Hz and SPL and PK is calculated on an unweighted field, the exclusion of higher frequencies does not affect the accuracy of the levels in these metrics.

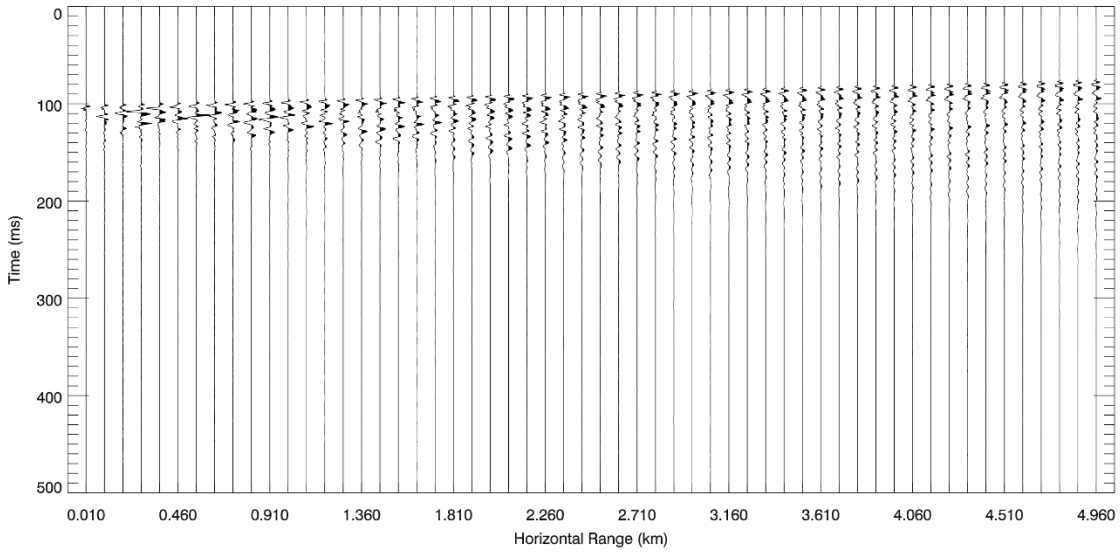

Figure 5. Example of synthetic pressure waveforms computed by FWRAM.

2.2.3. *N*×2-D Volume Approximation and Maximum-over-depth Sampling

The sound propagation models employed for this project are limited to two-dimensional (2-D) acoustic propagation. The calculations of the acoustic fields in three dimensions is achieved by propagating the acoustic field within 2-D vertical planes aligned along radials covering a 360° swath from the source, an approach commonly referred to as *N*×2-D. These vertical radial planes are separated by an angular step size of $\Delta\theta$, yielding $N = 360°/\Delta\theta$ number of planes (Figure 6).

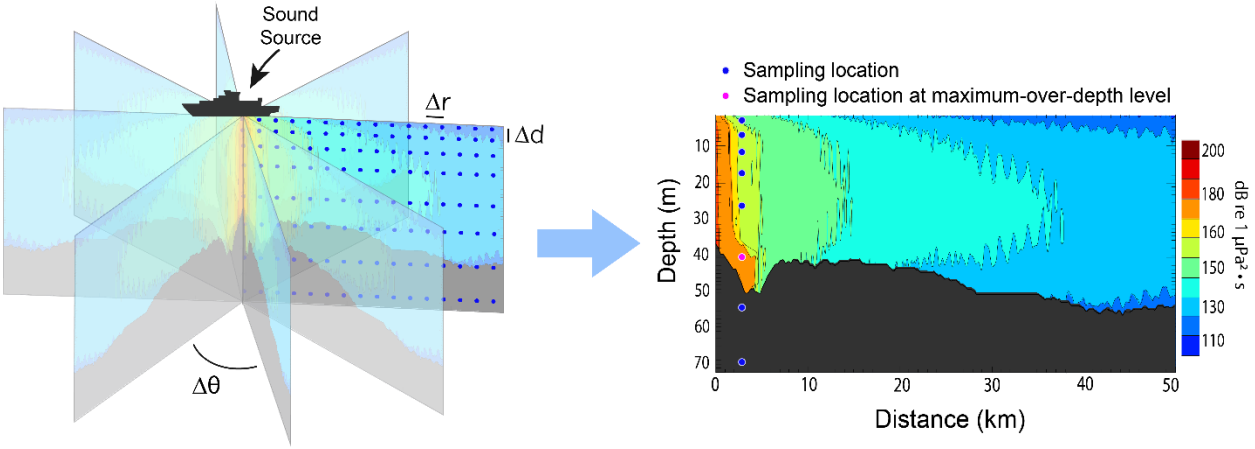

Figure 6. The *N*×2-D and maximum-over-depth modelling approach.

The received sound field within each vertical radial plane is sampled at various ranges from the source, generally with a fixed radial step size (Δr in Figure 6). At each sampling range along the surface, the sound field is sampled at various depths (Δd in Figure 6), with the step size between samples increasing with depth below the surface. The step sizes are chosen to provide increased coverage near the depth of the source and at depths of interest in terms of the sound speed profile. For areas with deep water, sampling is not performed at depths beyond those reachable by marine mammals. The received acoustic levels at a surface sampling location is taken as the maximum value that occurs over all samples within the water column, i.e., the maximum-over-depth received level. These maximum-over-depth acoustic levels are further used to calculate the ranges to specific thresholds and create acoustic field maps.

2.2.1. Calculating Isopleth Contours and Ranges to Threshold levels from Acoustic Fields

The output from received level modelling after reducing the vertical dimension using maximum-over-depth rule is a series of data points along radials originating at the source, i.e., in polar coordinates system. The data are interpolated onto a Cartesian grid. The isopleth contours and ranges to specific thresholds are both calculated from the acoustic field grids.

For the threshold level ranges, two distances relative to the source are reported: 1) R_{max}, the maximum range to the given sound level over all azimuths, and 2) $R_{95\%}$, the range to the given sound level after 5% of the farthest points were excluded (see examples in Figure 7).

The $R_{95\%}$ is used because sound field footprints are often irregular in shape. In some cases, a sound level contour might have small protrusions or anomalous isolated fringes. This is demonstrated in the image in Figure 7(a). In cases such as this, where relatively few points are excluded in any given direction, R_{max} can misrepresent the area of the region exposed to such effects, and $R_{95\%}$ is considered more representative. In strongly asymmetric cases such as shown in Figure 7(b), on the other hand, $R_{95\%}$ neglects to account for significant protrusions in the footprint. In such cases R_{max} might better represent the region of effect in specific directions. Cases such as this are usually associated with bathymetric features affecting propagation. The difference between R_{max} and $R_{95\%}$ depends on the source directivity and the non-uniformity of the acoustic environment.

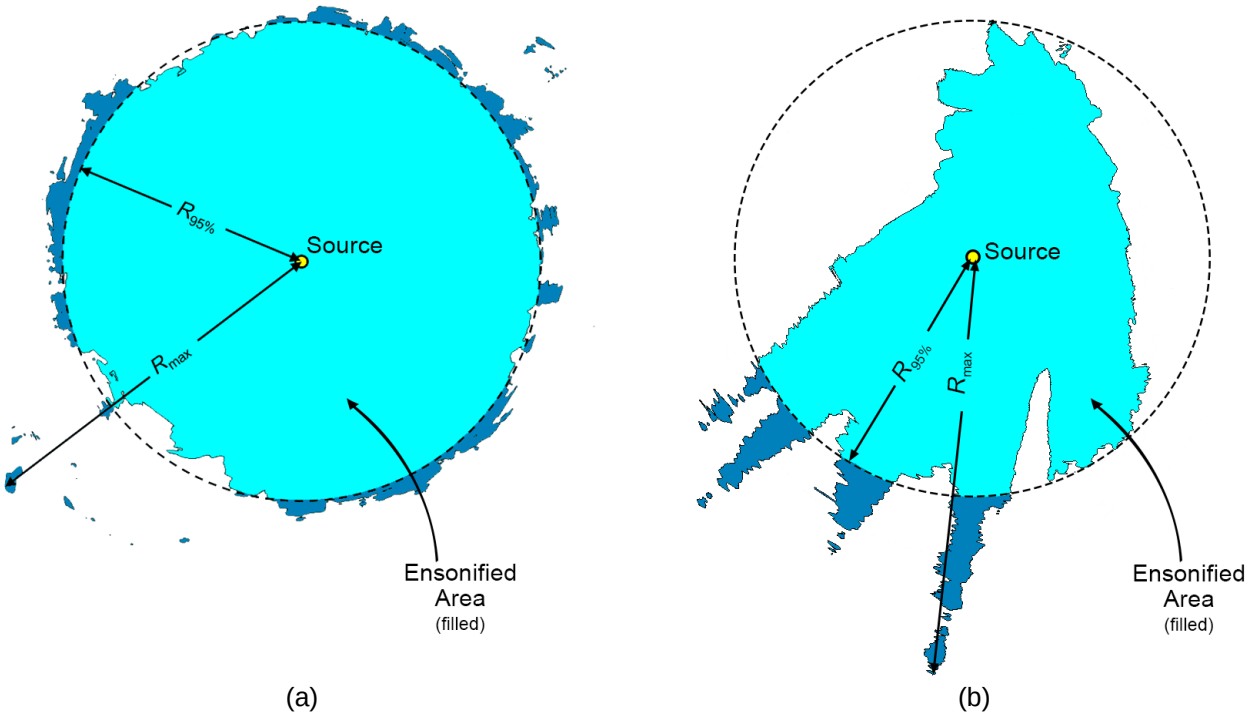

Figure 7. Sample areas ensonified to an arbitrary sound level with R_{max} and $R_{95\%}$ ranges shown for two contrasting scenarios. (a) a largely radially symmetric sound level contour with small protrusions, for which $R_{95\%}$ best represents the ensonified area; and (b) a strongly asymmetric sound level contour with long protrusions, for which R_{max} best represents the ensonified areas in some directions. Light blue indicates the ensonified areas bounded by $R_{95\%}$; darker blue indicates the ensonified areas beyond $R_{95\%}$ that determine R_{max}.

3. Model Parameters

3.1. Environmental Parameters

The water depths within the project area range from 60 to 200 m. Modelling site A was selected within project area (see Table 1) to be typical of a site of planned Suncor drilling operations. Figure 1 shows the site location. For the purpose of the cumulative sound field study, five additional source locations were also included; these are also listed in Table 1 and shown in Figure 2. Note that Site A is only a typical representative location for the planned activities of the Tilt Cove project, while S2–S6 are known locations of existing operations.

Table 1. Locations of sources that were used for modelling.

Designation	Geographic coordinates	UTM coordinates (Zone 22 North)	Water depth at source (m)
Site A – Suncor Project	46° 32' 46" N 48° 37' 6" W	682579E 5157498N	84
S2: Hibernia	46° 44' 36" N, 48° 47' 3" W	669262E 5179026N	77
S3: Hibernia Southern Ext.	46° 41' 25" N, 48° 45' 14" W	671744E 5173191N	82
S4: Hebron	46° 32' 29" N, 48° 30' 4" W	691592E 5157248N	93
S5: Terra Nova	46° 28' 27" N, 48° 29' 22" W	692719E 5149802N	97
S6: White Rose	46° 47' 19" N, 48° 1' 0" W	727704E 5186005N	130

3.1.1. Bathymetry

Water depths throughout the modelled area were obtained from digital bathymetry grid SRTM15+ (Smith and Sandwell 1997, Becker et al. 2009). The bathymetry grid has a resolution of 15 arc-seconds (~ 330 × 460 m at the studied latitude). The data were extracted for a 600 × 400 km area and re-gridded onto a Universal Transverse Mercator (UTM) Zone 22 coordinate projection with a regular grid spacing of 200 × 200 m.

3.1.2. Geoacoustics

The geoacoustic properties of surficial layers depend on the sediment type. As the porosity decreases, the compressional sound speed, sediment bulk density, and compressional attenuation increase. For each modelled location, MONM assumes a single geoacoustic profile of the seafloor for the entire modelled area.

MONM used these geoacoustic properties of the sediments:

- Bulk density (g/cm^3),
- Compressional-wave (or P-wave) speed (m/s),
- P-wave attenuation in decibels per wavelength (dB/λ),
- Shear-wave (or S-wave) speed (m/s), and
- S-wave attenuation in decibels per wavelength (dB/λ).

The surficial sedimentology in the area of the Jeanne D'Arc Basin, on the northwestern Grand Banks offshore Newfoundland, has been documented by numerous investigators. The generic geoacoustic

profile representing this area (see Table 2) was developed from information reported by Mosher and Sonnichsen (1992), King and Sonnichsen (2000), Divins (2010) and Abid et al. (2004). The geological stratification is composed of a surficial layer of sand and gravel, which overlays an acoustically-reflective layer of silty to fine sand. It is also characterized by a shallow acoustic basement of unconsolidated tertiary sediment extending for tens of kilometres below the seafloor. Following this profile, the geoacoustic parameters were estimated based on values reported by Ellis and Hughes (1989) and Osler (1994).

Table 2. Geoacoustic properties of the sub-bottom sediments as a function of depth, in meters below the seafloor (mbsf). Within each depth range, each parameter varies linearly within the stated range.

Depth (mbsf)	Material	Density (g/cm³)	P-wave speed (m/s)	P-wave attenuation (dB/λ)	S-wave speed (m/s)	S-wave attenuation (dB/λ)
0–5	Sand and gravel	1.9 to 2.0	1900 to 2000	0.36 to 0.47	200	2.0
5–50	Silty sand to fine sand	1.8 to 2.0	1650 to 1900	0.66 to 0.47		
50–255	Sand to sandy till	2.0 to 2.1	1900 to 2000	0.47 to 1.0		
> 255	Tertiary bedrock	2.2	2100	0.21		

3.1.3. Sound Speed Profiles

The sound speed profiles for the modelled sites were derived from temperature and salinity profiles from the U.S. Naval Oceanographic Office's *Generalized Digital Environmental Model V 3.0* (GDEM; Teague et al. 1990, Carnes 2009). GDEM provides a climatology data of temperature and salinity for the world's oceans as a latitude-longitude grid with 0.25° spatial resolution, with a temporal resolution of one month, based on global historical observations from the U.S. Navy's Master Oceanographic Observational Data Set (MOODS). The climatology profiles include 78 fixed-depth points to a maximum depth of 6,800 m (where the ocean is that deep). The GDEM temperature-salinity profiles were converted to sound speed profiles according to the equations of Coppens (1981):

$$\begin{aligned} c(z,T,S,\phi) &= 1449.05 + 45.7t - 5.21t^2 - 0.23t^3 \\ &\quad + \left(1.333 - 0.126t + 0.009t^2\right)\left(S - 35\right) + \Delta \\ \Delta &= 16.3Z + 0.18Z^2\,, \quad Z = \frac{z}{1000}\left[1 - 0.0026\cos\left(2\phi\right)\right], \quad t = \frac{T}{10} \end{aligned} \tag{13}$$

where z is water depth (m), T is temperature (°C), S is salinity (psu), and ϕ is latitude (radians).

Twelve monthly average sound speed profiles were calculated based on the data extracted from GDEM database for the modelling location (Figure 8, left). Out of this set, February and August were selected represent the range of acoustic propagation conditions that may occur during drilling operations (Figure 8, right), they are also representative of winter and summer, respectively.

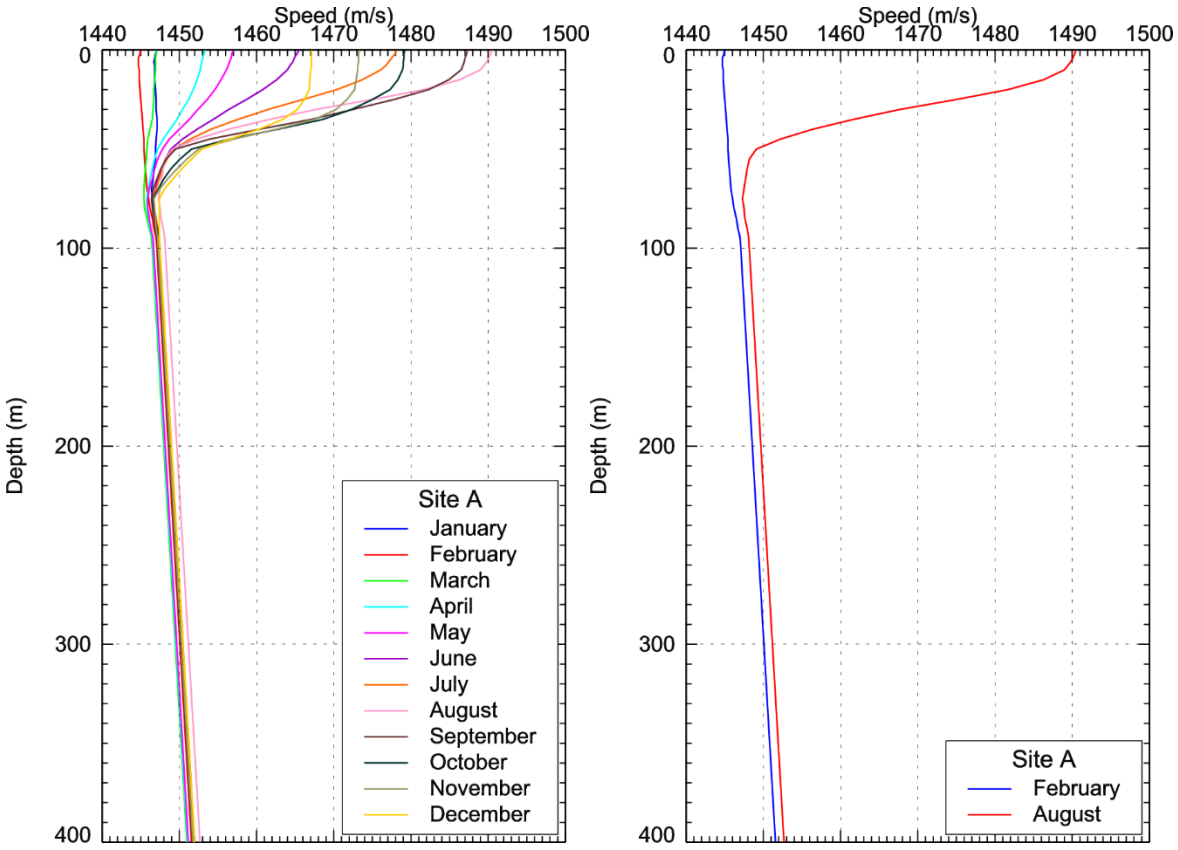

Figure 8. Mean monthly sound speed profiles near the modelling area: (left) twelve months and (right) two months selected for modelling (February, August). The profiles were derived from data obtained from *GDEM V 3.0* (Teague et al. 1990, Carnes 2009).

3.2. Geometry and Modelled Volumes

The modelling geometry for each source was selected individually based on the parameters of the source and the required output (Table 3). At each surface sampling location, the sound field was sampled at the bottom and at the following depths:

- 2 m,
- Every 5 m from 5 to 25 m,
- Every 25 m from 50 to 100 m,
- Every 50 m from 150 to 500 m,
- Every 100 m from 600 to 1000 m, and
- Every 200 m from 1200 to 2400 m.

Table 3. Modelling geometry for the individual sources.

Source	Metric	N-profiles (Azimuthal step)	Horizontal resolution (m)	Maximum distance (km)
Airgun array	SEL	72 (5°)	20	100
Airgun array	SPL and PK	36 (10°)	10	20
Vessel and MODU	SEL and SPL	72 (5°)	20	100

3.3. Acoustic Source Parameters and Modelled Source Levels

3.3.1. Representative VSP Source Airgun Array

The VSP modeling includes an airgun array: model name Dual Delta. The Dual Delta airgun array consists of three airguns of 250 in³ and three airguns of 150 in³ volume for a total of six airguns and 1200 in³ volume. The layout of the array is presented in Figure 9, where each set of three airguns is arranged in a vertical equilateral triangle. For the purpose of modeling, the horizontal axis of the array, which goes through the centre of each triangle, is placed at the expected operational depth of 5 m. The Dual Delta 1200 in³ array was modeled with a firing pressure of 2000 psi.

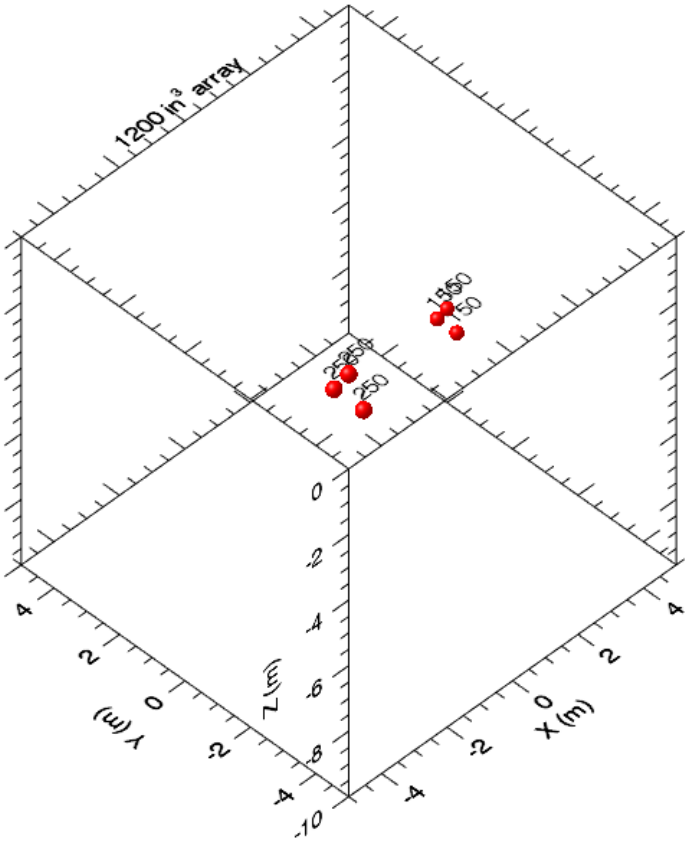

Figure 9. Geometry of the Dual Delta 1200 in³ airgun array. The large spheres represent the 250 in³ airguns and the small spheres represent the 150 in³ airguns

The AASM (see Section 2.1) was used to characterize the spectral attributes of the array's composite pressure signature in all directions. The horizontal overpressure signature and corresponding power spectrum level for the Dual Delta 1200 in³ array were computed at frequencies from 10 Hz to 25 kHz. These are shown in Figure 10 for the broadside (perpendicular to the tow direction) and endfire (parallel to the tow direction) directions up to 2 kHz. The broadband (10 Hz to 25 kHz) source levels are SEL of 218.1 dB re 1 µPa² s m broadside, 217.5 dB re 1 µPa² s m endfire, and SPL of 220.4 dB re 1 µPa m broadside, and 220.2 dB re 1 µPa m endfire based, on far-field horizontally propagating sound.

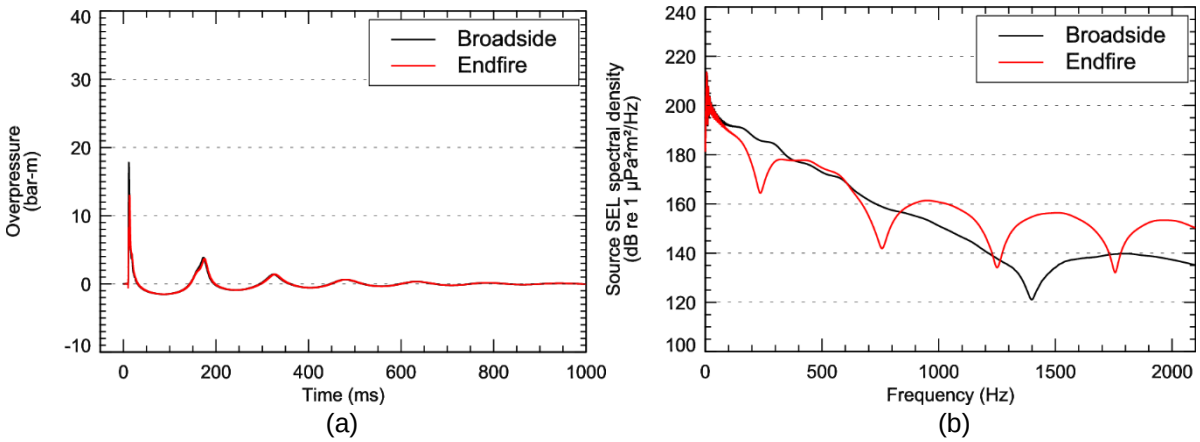

Figure 10. Predicted (a) overpressure signature and (b) power spectrum in the broadside and endfire (horizontal) directions for the Dual Delta 1200 in^3 airgun array.

The general trend for the spectral levels is to decrease with increasing frequency. Most of the acoustic wave energy (93%) is contained in frequency bands below 100 Hz. The signatures consist of a strong primary peak related to the initial firing of the airgun, followed by a series of pulses associated with bubble oscillations spaced at about 160 ms. Figure 11 shows the horizontal 1/3-octave-band directivities for the array. In this plot, the arrow indicates the tow direction of the array and the solid black curves indicate SEL source levels in dB re 1 µPa²m²s, as a function of angle in the horizontal plane.

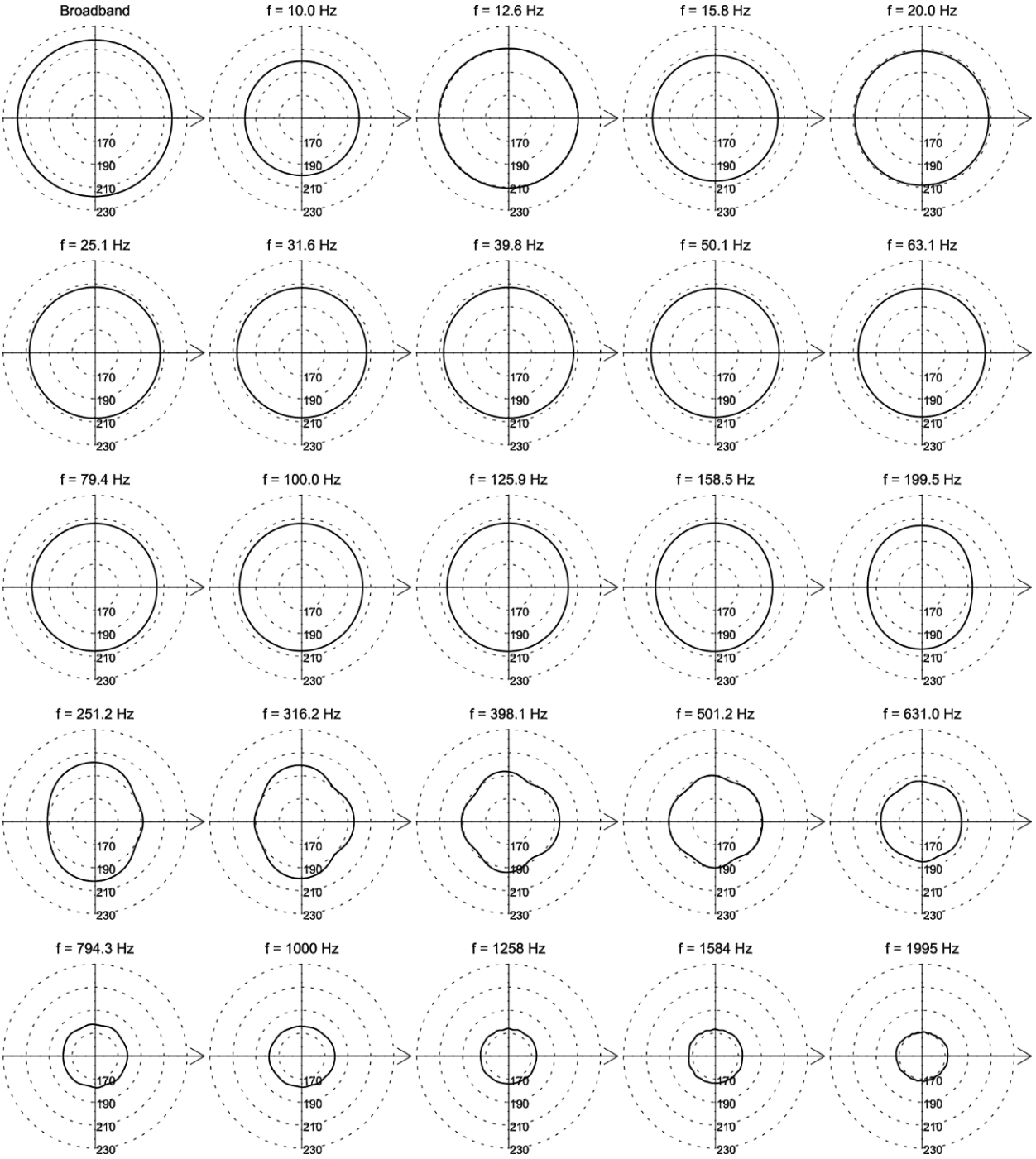

Figure 11. Directionality of predicted horizontal SEL source levels (SL, dB re 1 µPa²m²s) in 1/3-octave-bands for the modeled Dual Delta 1200 in^3 airgun array , at the 5 m tow depth. The 1/3-octave-band centre frequency is indicated above each plot.

3.3.2. Representative Drilling Platform and Support Vessel

A semi-submersible rig generates much more sound in the water, especially when used in a dynamic positioning (DP) assist anchored configuration as envisioned for the Suncor project. In principle, the total sound field generated underwater includes the sum of the contributions from all the noise sources. Where sources of comparable magnitude consistently operate in close proximity to each other, such as a set of thrusters on a vessel, or a set of airguns in an array, they must be modelled as a combined source. In other cases where the individual sources are typically at varying distances from each other, and where they are usually far enough apart that the more intense zones of potentially harmful sounds of their individual sound fields do not significantly overlap, it is sufficient to model the sources individually. Such cases include multiple support vessels servicing a drilling platform. Modelling these sources individually is always the first step in any such study. If it is then found that multiple sources have consistently overlapping zones of potentially harmful sound, it would be necessary to take the further step of combined source modelling. This is not typically the case for multiple support vessels and a drilling platform or drilling vessel, and in this case, separately modelling one support vessel along with the drilling platform or drilling vessel gives an accurate assessment of the environmental consequences of the complete operation, without the need to jointly model the combined sound field of the multiple sources.

The highest sound levels from MODU and vessels while in DP are generated by the propellers. Thus, source levels associated with drill rigs and support vessels are often estimated based on a platform's propulsion system. The specific parameters required as modelling input for each vessel are:

- Thruster depth,
- Propeller diameter,
- Propeller revolutions-per-minute (rpm) at nominal power output, and
- Number of blades.

Our modelling assumes that the MODU will use DP assist to maintain position, while being anchored at the drill site. Therefore, the thrusters on the MODU will be the main sound source at the site. To estimate the sound produced while in DP assist anchored mode, we assume the sound produced by only 4 of the 8 thrusters in continuous operation.

Sound levels are generally lower during drilling operations than during other operations such as maintenance, station keeping during bad weather, or during transits. This is because the mechanical activities specifically involved in drilling do not generate very much sound in the water as compared to the sound generated by a propeller turning in the water at high speed; the tips of the propeller blades push the water with such force that it briefly tears small holes in the water in a process known as propeller cavitation; the water quickly snaps back to refill those little voids of vacuum, making a loud sound for each such event, of which there are a great many in rapid succession, thereby generating intense cavitation noise.

3.3.2.1. Semi-Submersible Platform

The estimates of the semi-submersible platform acoustic source levels and sound spectrum were based on the *Seadrill West Sirius* (Figure 12). *Seadrill West Sirius* is reportedly equipped with eight Rolls-Royce UUC 355 thrusters. The thruster has a fixed-pitch propeller in a PV-nozzle. For modelling the DP-assist anchored configuration, four of the eight thrusters were assumed to operate at nominal speed. The vertical position of the thrusters was 18 m below the sea surface (draft of the rig during drilling operations). Figure 13 shows the thruster locations.

The parameters for the UUC 355 thruster are:

- 3.5 m propeller diameter,
- 177 rpm nominal propeller speed, and
- 3800 kW maximum continuous power input.

Figure 12. *Seadrill West Sirius* semi-submersible platform.

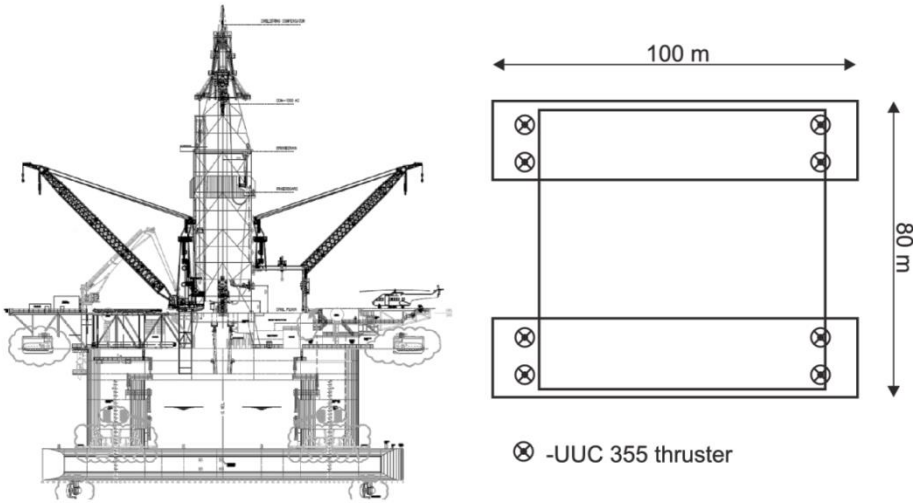

Figure 13. *Seadrill West Sirius* dimensions and thruster locations (circles).

The vertical position of the thrusters below the sea surface during drilling operations is a function of the draft of the vessel, since the thrusters are located at the very bottom, under the deepest floatation element of the structure. The specifications for the *Seadrill West Sirius* give a range of draft during operations between 18–20 m. For the present modelling, we assigned the acoustic source depth of the semi-submersible platform to be 18 m.

As described in Section 2.1.2, a hybrid approach for defining the source levels for the *Seadrill West Sirius* drilling platform was used. For modelling the source level, four of the eight thrusters (combined maximum power 30,400 kW) were assumed to be operating on average, in DP-assist mooring, so effectively 50% of maximum power. The source levels and the sound spectrum (Figure 14, red line) for cavitating thrusters were estimated based on the *Seadrill West Sirius* thruster specifications (diameter and rpm) according to the method described in Section 2.1.2.1, using Equation 6. Table 4 lists the broadband source levels for a single UUC355 thruster operating at 100%, as well as four and eight thrusters. For the purpose of acoustic propagation modelling, all the thrusters were assumed to be located at the same spot, i.e., represented by a point source.

Table 4. Estimated broadband levels for cavitating thrusters used on the *Seadrill West Sirius*.

Source	Power output (% of nominal)	SPL (dB re 1 µPa m)
UUC355	100	187.7
8 × UUC355	100	196.7
4 × UUC355	100	193.7

The source level spectrum calculated for a cavitating propeller was combined with the source levels defined using a surrogate vessel by scaling the surrogate spectrum so that it matches the broadband level of the *Seadrill West Sirius* thruster sound emissions. The surrogate vessel used was another semi-submersible platform, the *Polar Pioneer*. It is reportedly equipped with four Liaan TNCP 105/75–280 rated at 2,400 kW azimuthing. Although detailed specifications on this thruster are not readily available, JASCO previously obtained field measurements of the *Polar Pioneer* underwater sound spectrum while transiting under DP thruster power at 6.4 kts—with a broadband (10 Hz to 35 kHz) source level of 196.8 dB re 1 µPa m (Austin and Li 2016). The shape of the *Polar Pioneer* underwater sound spectrum under transit is a good surrogate for the shape of the *Seadrill West Sirius* underwater sound spectrum under DP-assist anchored drilling operations. That spectrum was scaled in power so that the broadband level of the scaled spectrum matches the broadband level of the *Seadrill West Sirius* DP-assist anchored operations (193.7 dB re 1 µPa m)—i.e., the Polar Pioneer transiting spectrum was reduced by 3.1 dB to become the estimated *Seadrill West Sirius* DP-assist anchored drilling operations spectrum.

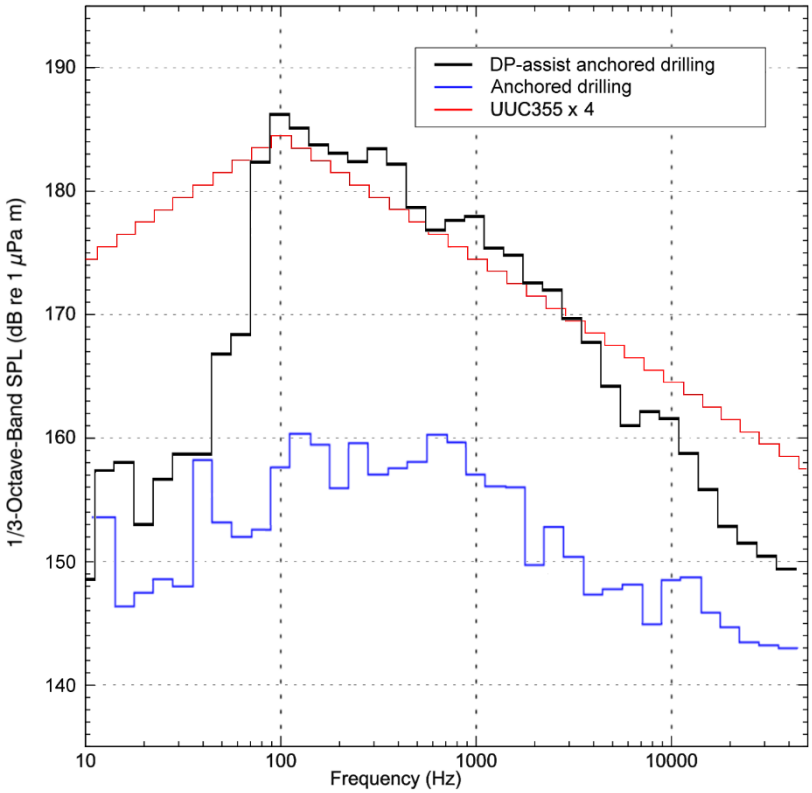

Figure 14. Source level spectrum assumed for the semi-submersible *Seadrill West Sirius* under DP-assist anchored drilling operations (black line). The source level spectrum for four UUC355 thrusters operating at capacity (red line) and the anchored (no DP assist) drilling radiated underwater sound for the surrogate vessel, *Polar Pioneer* (blue line), are also shown.

Although the thrusters often dominate the noise spectrum, especially in the lower frequency band (below 500 Hz), they are not the only source of sound from the semi-submersible platform operations. There is also machinery noise, which is transmitted through the structure and projected into the water by hull vibrations, albeit not very efficiently in the case of semi-submersibles. JASCO also previously obtained field measurements of the *Polar Pioneer* underwater sound spectrum while drilling under mooring—with a broadband (10 Hz to 35 kHz) source level of 170.1 dB re 1 µPa m (Austin et al. 2018). Since the thrusters are not used (very much) during moored operations, these measurements of the *Polar Pioneer* drilling operations are a good surrogate for the machinery noise component of the *Seadrill West Sirius* underwater sound spectrum during drilling operations. As described for this hybrid method, the maximum of the two spectra are taken in each decidecade (or 1/3-octave) band. As it turns out, the thruster noise is higher than the radiated machinery noise in every band.

3.3.2.2. Representative Support Vessel: DSV Fu Lai

Offshore standby safety vessels are typically ~50–100 m long, 10–20 m wide, with a 3–8 m draft. They are usually fitted with bow and stern thrusters or propellers, and a dynamic positioning system.

For this work we have used the DSV *Fu Lai* (Figure 15) as a representative vessel of this class to simulate the source level spectrum of a typical standby safety vessel. The measured broadband level of this vessel was used to scale a generic source spectrum. The DSV *Fu Lai* is 107 m long with a total drive power of 12800 HP. Although it is technically a dive support vessel, its acoustic characteristics are primarily a function of its propulsion system, and in this way it is equivalent to more typical offshore supply vessels and drilling support vessels. The main reason for using it as a representative vessel of this class is that source measurements are available for use in this study. The acoustic signature of this vessel (broadband level of 178 dB re 1 µPa m) was recorded by JASCO in dynamic positioning mode at 20–30% power (MacGillivray 2006). For the purpose of the current modelling, a generic version of the source spectrum was derived based on scaling the measured broadband level, so the SL spectrum is less specific to the particular vessel and more representative of the general case. The derived 1/3-octave band SL spectrum is plotted in Figure 16.

Figure 15. Support vessel *Fu Lai*, used to represent a typical standby safety vessel for acoustic modelling.

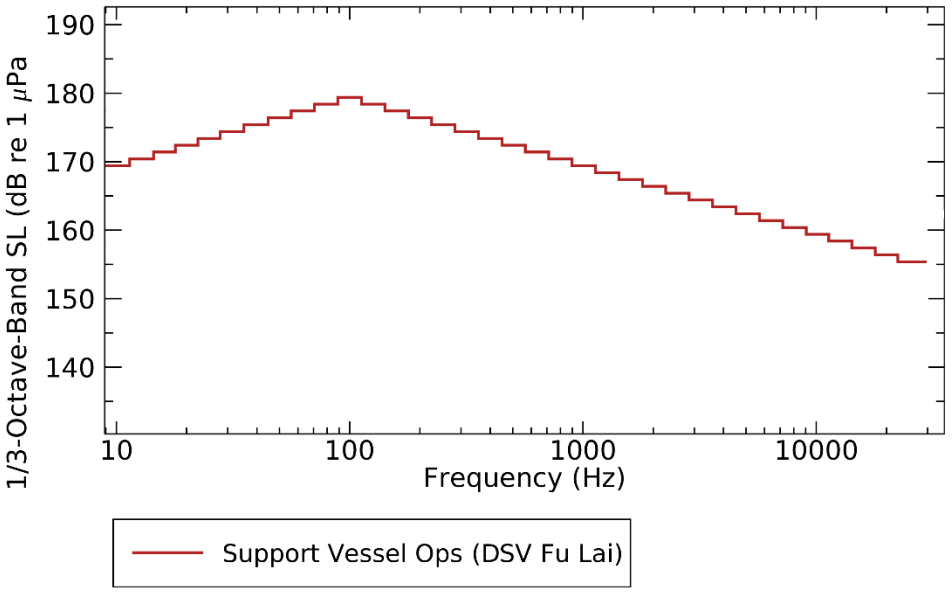

Figure 16. Source level spectrum, as 1/3-octave band levels, for support vessel DSV *Fu Lai*, used to represent a typical standby safety vessel for acoustic modelling.

3.3.2.3. Summary of modelled vessel source levels

The general modelling parameters of the two thruster-based sources, and the methods by which they were derived, are summarized in Table 5.

Table 5. Summary of modelled vessel sources.

Source	Method used to obtain spectrum	Method used to obtain broadband SL	Broadband SL (dB re 1 µPa m)	Source depth (m)
Semi-submersible drill rig *Seadrill West Sirius*	Max. of (a) scaling measured DP spectrum to broadband thrusters SL, and (b) measured surrogate moored machinery noise.	Thruster power formula	193.7	18
Support vessel *Fu Lai*	Scaling generic spectrum to broadband SL	Field measurements	178	5

4. Acoustic Field Modelling Results

Two types of acoustic field metrics were modelled for each source: SPL and cumulative SEL; PK was also modelled for the seismic source. The modelled fields were assessed against the criteria thresholds defined in NMFS (2018).

Maps of the horizontal acoustic field footprints were plotted, and the ranges to specific thresholds were calculated based on a 2-D Cartesian grid representing horizontal distribution of the acoustic field around a source (see Section 2.2.1). The vertical dimension was reduced using the maximum-over-depth rule (see Section 2.2.3).

4.1. Seismic Survey Source

The Dual Delta 1200 in^3 airgun array was modelled at single site. The modelling was performed using the sound speed profile representing typical propagation conditions for February and August. The seismic source will be deployed from or near the drilling platform and was assumed to be stationary for the duration of the survey. For the purpose of calculating SEL_{24h}, it was assumed that the maximum number of seismic pulses delivered within a 24 hr period is 363.

4.1.1. SPL and PK

The SPL and peak sound pressure level (PK) for the seismic source were estimated based on the full waveform modelling (see Section 2.2.2). The modelling was performed along 36 transects (10° regular angular steps) up to a 20 km range from the source for the frequencies from 9 to 891 Hz. The SPL and PK were calculated directly from the synthetic pressure waveforms. The difference between SEL and SPL over this 20 km range was used to estimate a range-dependent function for converting SEL to SPL values, and this was used to estimate SPL out to a maximum range of 100 km, using the SEL field calculated by the MONM model.

The ranges to the specific thresholds for SPL are presented in Table 6. The injury thresholds (190 dB for pinnipeds and 180 dB for cetaceans) as well as the behavior response threshold for an impulsive sound source (160 dB) based on NMFS (2018) criteria (see Section B.1) are bolded.

Table 6. VSP 1200 in^3 airgun array: Maximum (R_{max}, km) and 95% ($R_{95\%}$, km) horizontal ranges from the source to modelled maximum-over-depth sound pressure level (SPL) thresholds. The PTS threshold for pinnipeds and cetaceans (190 dB and 180 dB, respectively) and TTS threshold for an impulsive source (160 dB) are in bold.

SPL (dB re 1 µPa)	February		August	
	R_{max}	$R_{95\%}$	R_{max}	$R_{95\%}$
210	0.010	0.010	0.010	0.010
200	0.022	0.022	0.022	0.022
190	**0.082**	**0.081**	**0.081**	**0.081**
180	**0.462**	**0.441**	**0.490**	**0.465**
170	1.95	1.80	2.05	1.91
160	**6.60**	**5.80**	**6.09**	**5.66**
150	19.19	16.64	16.65	14.56
140	40.5	36.0	33.5	29.3
130	84.2	72.4	65.3	55.9
120	>100*	n/c	>100*	n/c

* Extends beyond modelling boundary
n/c = not computed because R_{max} was not defined

The ranges to the criteria-defined PTS-onset thresholds for the PK are presented in Table 7. Examples of the vertical distribution of the SPL field are provided in Figures 17 and 18. A contour map of the maximum-over-depth SPL field around the source is provided in Figure 19.

Table 7. VSP 1200 in³ airgun array: Maximum (R_{max}, km) and 95% ($R_{95\%}$, km) horizontal ranges from the source to modelled PTS-onset thresholds defined for the PK field based on NMFS (2018).

Marine mammal group	Threshold (dB re 1 µPa)	February		August	
		R_{max}	$R_{95\%}$	R_{max}	$R_{95\%}$
NMFS (2018)					
Low-frequency cetaceans	219	0.014	0.014	0.014	0.014
Mid-frequency cetaceans	230	—	—	—	—
High-frequency cetaceans	202	0.121	0.120	0.121	0.117
Phocid pinnipeds (underwater)	218	0.014	0.014	0.014	0.014
Otariid pinnipeds (underwater)	232	—	—	—	—

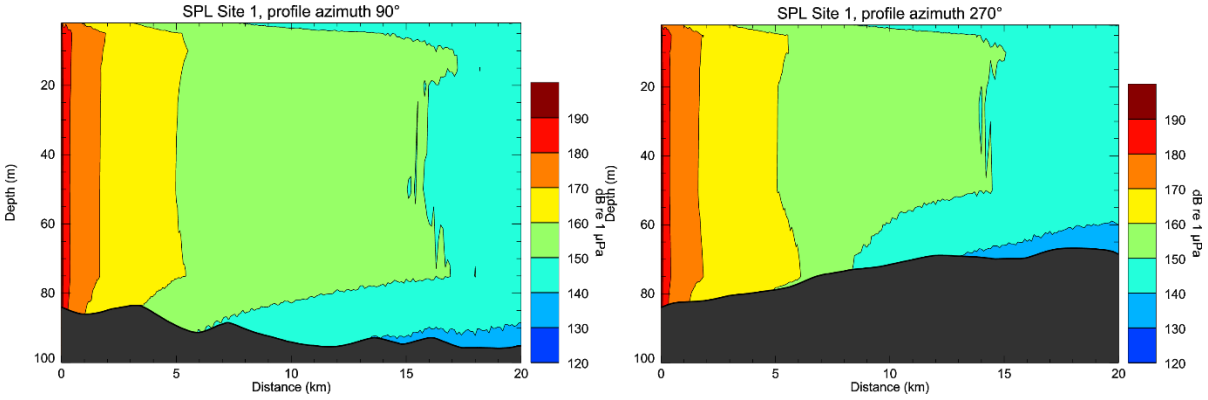

Figure 17. VSP 1200 in³ airgun array: Modelled vertical distribution of the sound pressure level (SPL) field for azimuth bearing 90° (left) and 270°(right) using the modelled profiles for February.

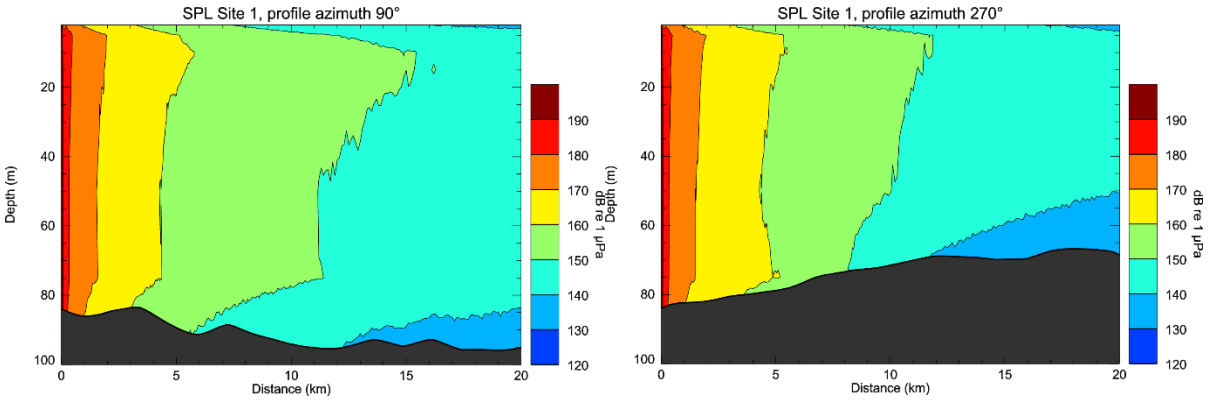

Figure 18. VSP 1200 in³ airgun array: Modelled vertical distribution of the sound pressure level (SPL) field for azimuth bearing 90° (left) and 270°(right) using the modelled profiles for August.

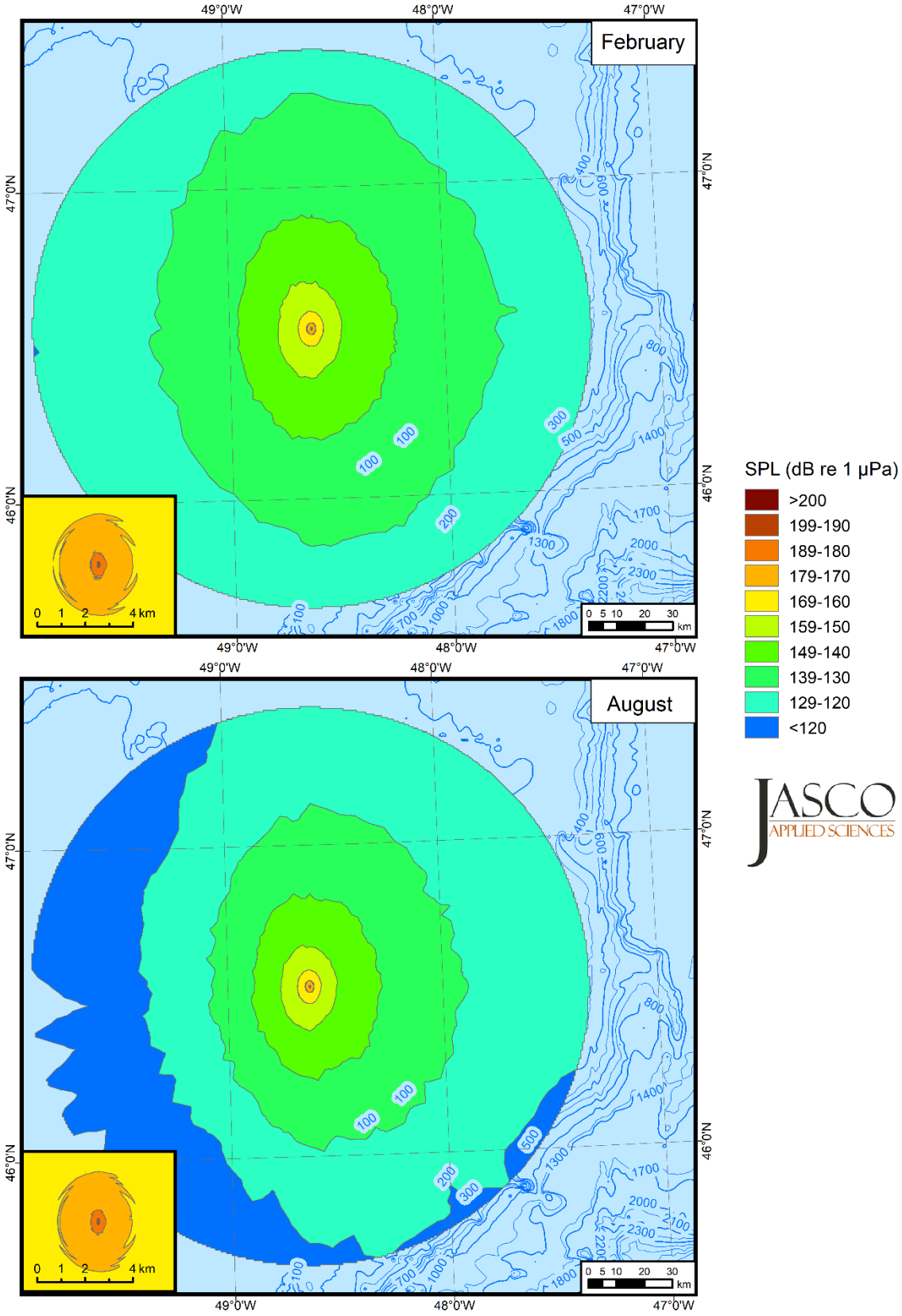

Figure 19. VSP 1200 in³ airgun array: Modelled maximum-over-depth sound pressure level (SPL) field, tow heading of 90°.

4.1.2. SEL

The per-pulse SEL field modelling was performed along 72 transects (5° regular angular step) up to a 100 km range from the source utilizing energy propagation loss in the decidecade band approach (Section 2.2.1). Bands with central frequencies from 10 to 25,000 Hz were considered. The ranges to specific thresholds based on unweighted per-pulse SEL field are provided in Table 8 and the threshold contour map in Figure 20.

The SEL_{24h} for the VSP source was calculated based on the per-pulse SEL with the assumption that the VSP source will be delivering a maximum of 363 pulses in a given 24 hr period. According to Equation A-4, the 363 pulses result in an increase in exposure by 25.6 dB over a single pulse exposure.

The SEL_{24h} field was assessed against impulsive source criteria for each marine mammal group defined in NMFS (2018) after application of specific M-weighting functions. The PTS-onset and TTS-onset threshold ranges based on the M-weighted SEL_{24h} field are provided in Table 9 and the PTS-onset threshold contour map is shown in Figure 21.

Table 8. VSP 1200 in³ airgun array: Maximum (R_{max}, km) and 95% ($R_{95\%}$, km) horizontal distances from the source to modelled unweighted 24-hour maximum-over-depth sound exposure level (SEL_{24}) isopleths.

SEL_{24} (dB re 1 µPa² s)	**February**		**August**	
	R_{max}	$R_{95\%}$	R_{max}	$R_{95\%}$
220	0.014	0.014	0.014	0.014
210	0.041	0.041	0.041	0.041
200	0.284	0.253	0.282	0.234
190	1.68	1.38	1.38	1.24
180	6.54	5.83	5.93	5.26
170	20.5	17.6	17.8	14.9
160	54.8	47.7	36.5	31.8
150	>100*	n/c	69.8	59.6
140	—	—	>100*	n/c
130	—	—	—	—
120	—	—	—	—

* Extends beyond modelling boundary
n/c = not computed because R_{max} was not defined
— = beyond modelling limits

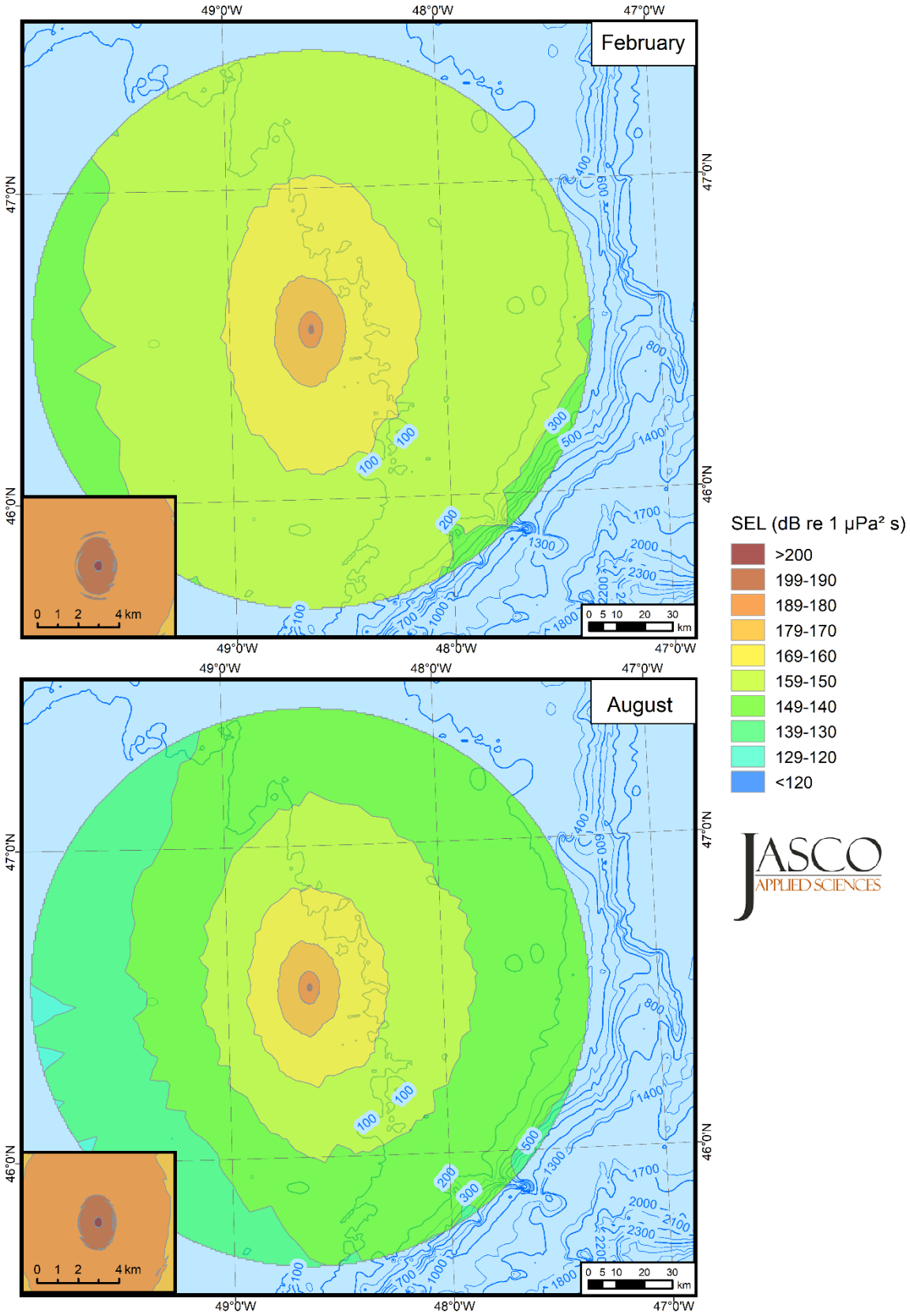

Figure 20. VSP 1200 in³ airgun array: Modelled 24-hour sound exposure level (SEL_{24}) field.

Table 9. VSP 1200 in³ airgun array: Maximum (R_{max}, km) and 95% ($R_{95\%}$, km) horizontal distances from the source to PTS-onset and TTS-onset thresholds NMFS (2018) based on the 24 hr M-weighted sound exposure level (SEL) field.

Marine mammal group	PTS-onset					TTS-onset				
	SEL (dB re 1 µPa²·s)	February		August		SEL (dB re 1 µPa²·s)	February		August	
		R_{max}	$R_{95\%}$	R_{max}	$R_{95\%}$		R_{max}	$R_{95\%}$	R_{max}	$R_{95\%}$
NMFS (2018)										
Low-frequency cetaceans	183	2.45	1.95	2.19	1.88	168	16.6	14.5	15.2	13.0
Mid-frequency cetaceans	185	< 0.010	< 0.010	< 0.010	< 0.010	170	0.014	0.014	0.014	0.014
High-frequency cetaceans	155	0.040	0.036	0.040	0.036	140	0.491	0.411	0.480	0.420
Phocid pinnipeds (underwater)	185	0.073	0.071	0.071	0.063	170	1.37	1.25	1.43	1.26
Otariid pinnipeds (underwater)	203	0.014	0.014	0.014	0.014	188	0.030	0.030	0.030	0.030

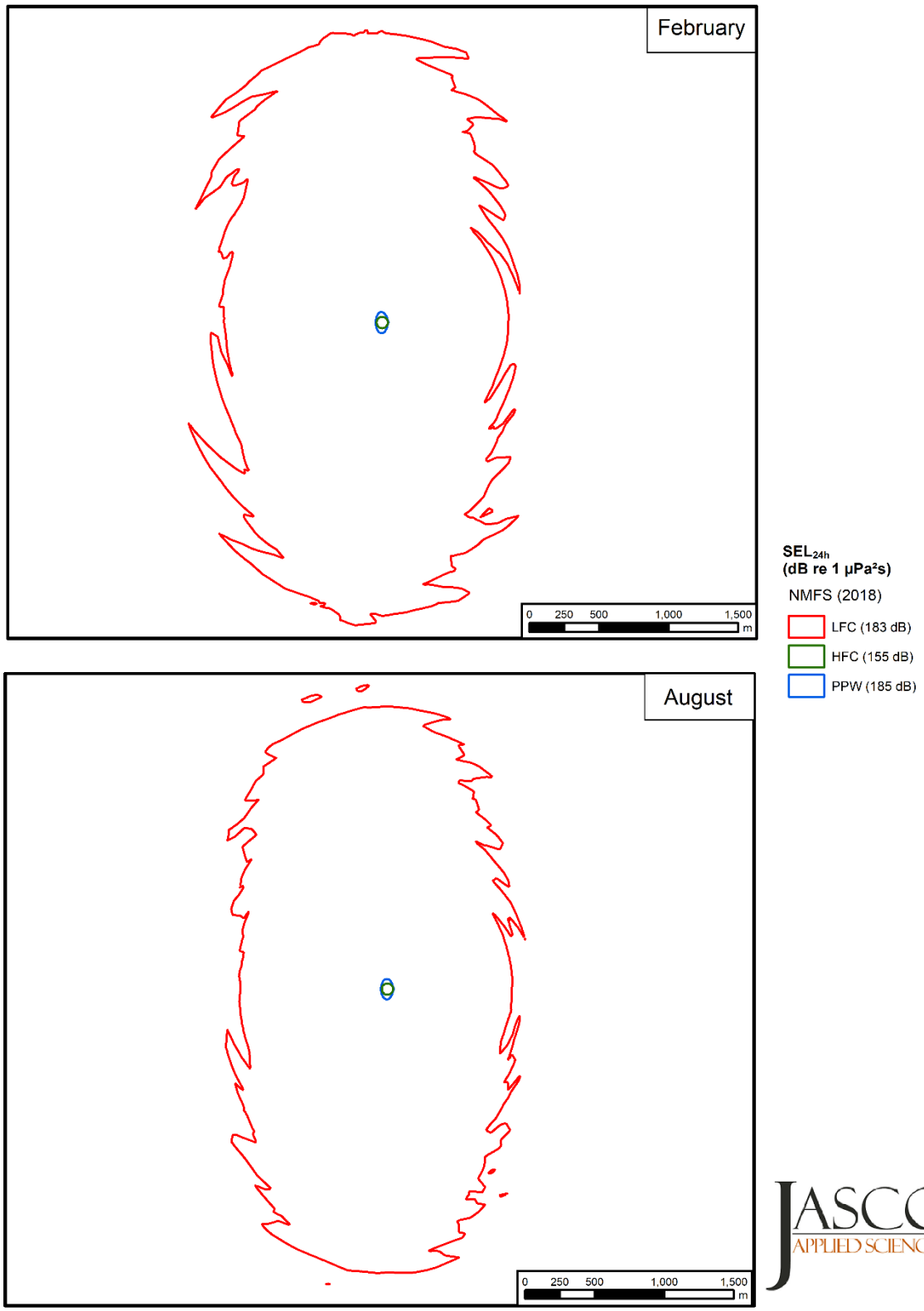

Figure 21. VSP 1200 in³ airgun array: PTS-onset threshold contours NMFS (2018) based on the 24 hr M-weighted sound exposure level (SEL_{24}) field.

4.2. MODU and Supply Vessel

The MODU and supply vessel operations were modelled at site A for the propagation conditions in February and August.

The source levels were designed to represent operation of the vessels with power output equivalent to operating four of the eight dynamic positioning thrusters. The modelling was performed for the frequency range from 10 to 25,000 Hz along 72 transects up to 100 km range from the source. For the simplicity of the interpretation, these sources were modelled as a point source.

4.2.1. SPL

The thruster-generated sound is non-impulsive or a continuous noise source. For continuous sources, SPL and SEL_{1s} are equivalent because the integration time for the purpose of the SPL calculations is taken as 1 second. Therefore, the SPL field for continuous sources can be estimated using propagation loss modelling approach (Section 2.2).

The underwater sound fields predicted by the propagation models were sampled such that the received sound level at each point in the horizontal plane was taken to be the maximum value over all modelled depths for that point (Section 2.2.3). The resultant maximum-over-depth SPL fields are presented below in two formats: as tables of distances to sound levels and as contour maps showing the directivity and range to various sound levels.

The predicted distances to specific levels were computed from the maximum-over-depth sound fields. Two distances, relative to the source, are reported for each sound level: (1) R_{max}, the maximum range at which the given sound level was encountered in the modelled maximum-over-depth sound field, and (2) $R_{95\%}$, the maximum range at which the given sound level was encountered after excluding 5% of the farthest such points.

The distances to the sound level thresholds from 210 to 120 dB re 1 µPa SPL with 10 dB step are presented in Tables 10 and 11 for February and August propagation conditions. The injury thresholds (190 dB for pinnipeds and 180 dB for cetaceans) as well as the behavior response threshold for a non-impulsive sound source (120 dB) based on NMFS (2018) criteria (see Section B.1) are bolded. The contour maps of the estimated acoustic fields in SPL are presented in Figures 22 and 23.

Table 10. Semisubmersible (*Seadrill West Sirius*), Maximum (R_{max}, km) and 95% ($R_{95\%}$, km) horizontal distances from the source to modelled maximum-over-depth SPL thresholds. The injury thresholds (190 dB for pinnipeds and 180 dB for cetaceans) as well as the behavior response threshold for a non-impulsive sound source (120 dB) are bolded.

SPL (dB re 1 µPa)	February		August	
	R_{max}	$R_{95\%}$	R_{max}	$R_{95\%}$
190	**—**	**—**	**—**	**—**
180	< 0.014	< 0.014	< 0.014	< 0.014
170	0.014	0.014	0.014	0.014
160	0.078	0.076	0.081	0.076
150	0.522	0.496	0.607	0.475
140	3.47	3.00	3.79	3.12
130	18.0	16.3	14.4	13.3
120	**75.2**	**63.3**	**38.4**	**34.0**
110	>100*	n/c	86.2	74.2

* Extends beyond modelling boundary
n/c = not computed because R_{max} was not defined

Table 11. Support Vessel Ops (DVS *Fu Lai*), Maximum (R_{max}, km) and 95% ($R_{95\%}$, km) horizontal distances from the source to modelled maximum-over-depth SPL thresholds. The injury thresholds (190 dB for pinnipeds and 180 dB for cetaceans) as well as the behavior response threshold for a non-impulsive sound source (120 dB) are bolded.

SPL (dB re 1 µPa)	February		August	
	R_{max}	$R_{95\%}$	R_{max}	$R_{95\%}$
190	**—**	**—**	**—**	**—**
180	**< 0.014**	**< 0.014**	**< 0.014**	**< 0.014**
170	0.014	0.014	0.014	0.014
160	0.036	0.036	0.036	0.036
150	0.222	0.214	0.225	0.216
140	1.04	0.984	1.07	1.01
130	5.22	4.65	4.89	4.46
120	**17.7**	**16.5**	**15.9**	**14.6**
110	59.3	52.7	39.4	36.3

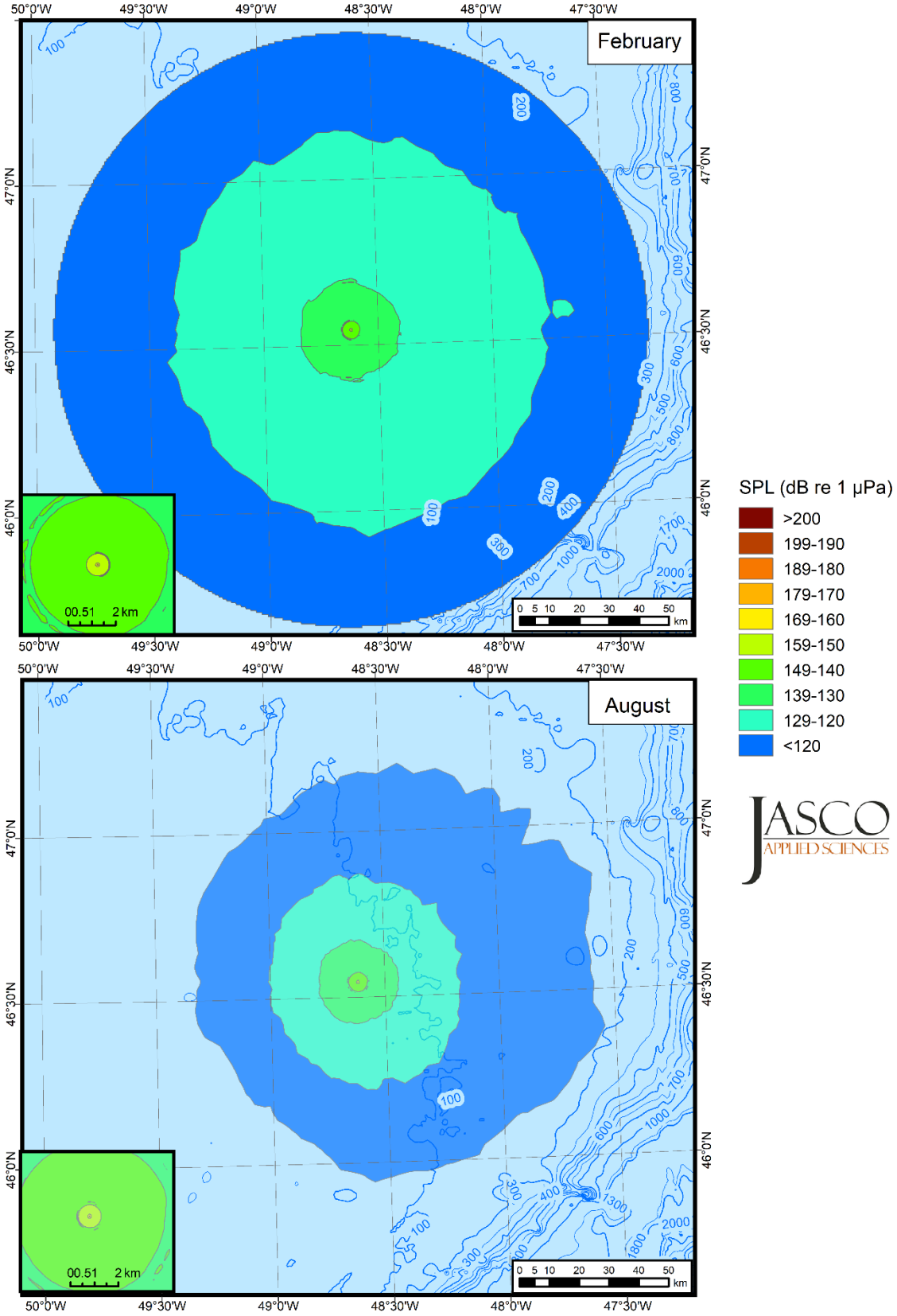

Figure 22. Semisubmersible (*Seadrill West Sirius*): Broadband (10–25,000 Hz) maximum-over-depth SPL field. Blue contours indicate water depth in metres.

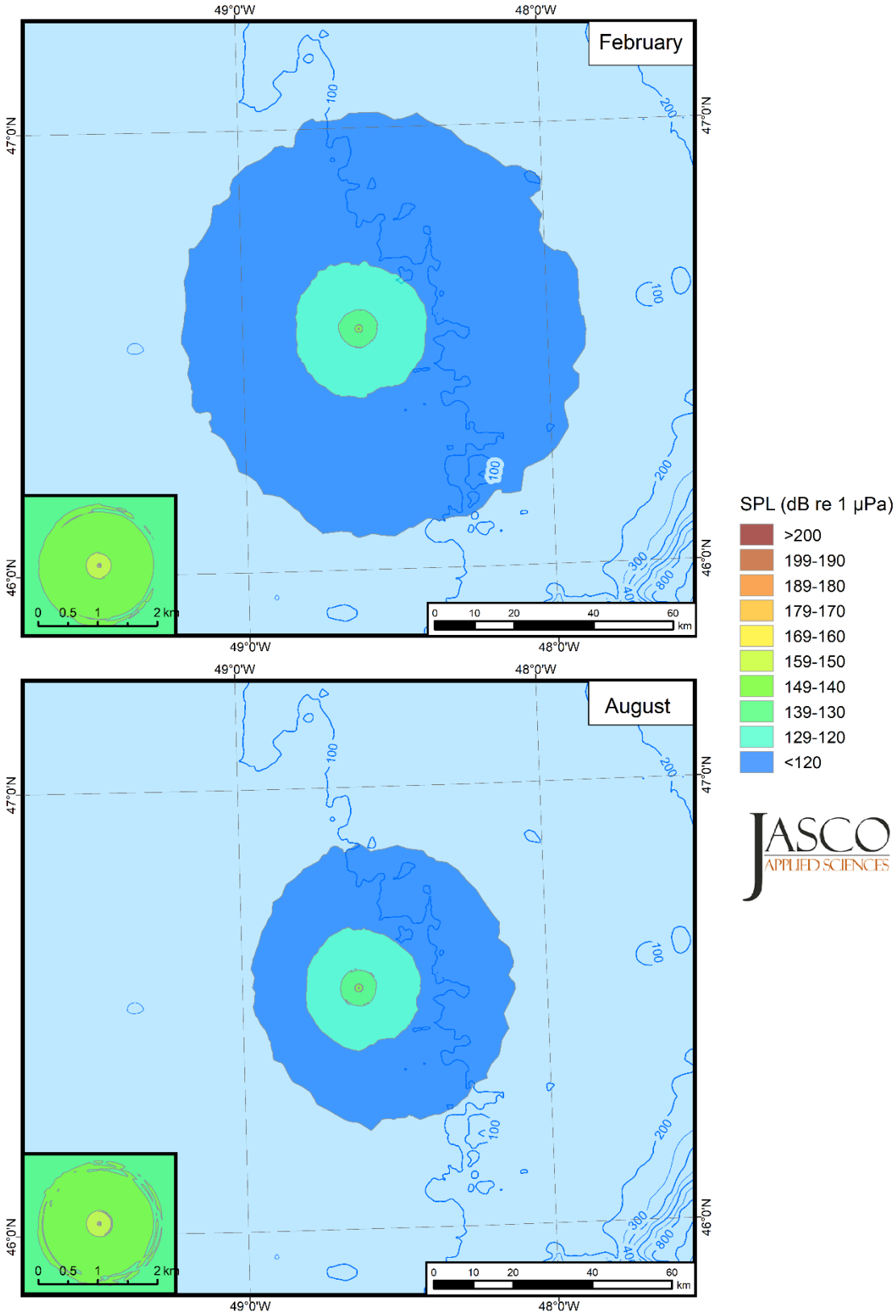

Figure 23. Support Vessel Ops (DVS *Fu Lai*): Broadband (10–25,000 Hz) maximum-over-depth SPL field. Blue contours indicate water depth in metres.

4.2.2. Sound Exposure Levels

For the purpose of the 24-hr SEL calculations it was assumed that the thruster-based sources are stationary, and the source levels do not change with time. The SEL_{24hr} was estimated from 1 sec SEL by adding 49.3 dB to account for the number of seconds in 24 hours (86,400 seconds).

The maximum ranges to the specific TTS- and PTS-onset thresholds were estimated for each marine mammal group using M-weighting functions as defined in NMFS (2018) for non-impulsive noise source. The calculations were performed for February and August propagation.

Table 12. *Seadrill West Sirius*; Safe distances in metres from the source to PTS- and TTS-onset thresholds NMFS (2018) based on the 24-hr SEL field.

Marine mammal group	PTS-onset					TTS-onset				
	SEL (dB re 1 µPa²·s)	February		August		SEL (dB re 1 µPa²·s)	February		August	
		R_{max}	$R_{95\%}$	R_{max}	$R_{95\%}$		R_{max}	$R_{95\%}$	R_{max}	$R_{95\%}$
NMFS (2018)										
Low-frequency cetaceans	199	0.364	0.345	0.365	0.351	179	12.2	11.1	10.0	9.93
Mid-frequency cetaceans	198	< 0.014	< 0.014	< 0.014	< 0.014	178	0.108	0.103	0.106	0.103
High-frequency cetaceans	173	0.142	0.139	0.149	0.143	153	3.83	3.60	4.78	4.46
Phocid pinnipeds (underwater)	201	0.036	0.036	0.036	0.036	181	1.40	1.18	1.96	1.84
Otariid pinnipeds (underwater)	219	< 0.014	< 0.014	< 0.014	< 0.014	199	0.045	0.045	0.051	0.051

Table 13. Support vessel; Safe distances in metres from the source to PTS- and TTS-onset thresholds NMFS (2018) based on the 24-hr SEL field.

Marine mammal group	PTS-onset					TTS-onset				
	SEL (dB re 1 µPa²·s)	February		August		SEL (dB re 1 µPa²·s)	February		August	
		R_{max}	$R_{95\%}$	R_{max}	$R_{95\%}$		R_{max}	$R_{95\%}$	R_{max}	$R_{95\%}$
NMFS (2018)										
Low-frequency cetaceans	199	0.073	0.072	0.073	0.072	179	3.65	3.29	3.96	3.50
Mid-frequency cetaceans	198	< 0.014	< 0.014	< 0.014	< 0.014	178	0.092	0.092	0.092	0.092
High-frequency cetaceans	173	0.136	0.134	0.142	0.139	153	3.07	2.91	3.94	3.66
Phocid pinnipeds (underwater)	201	0.020	0.020	0.020	0.020	181	0.405	0.366	0.433	0.385
Otariid pinnipeds (underwater)	219	0.010	0.010	0.010	0.010	199	0.030	0.030	0.032	0.032

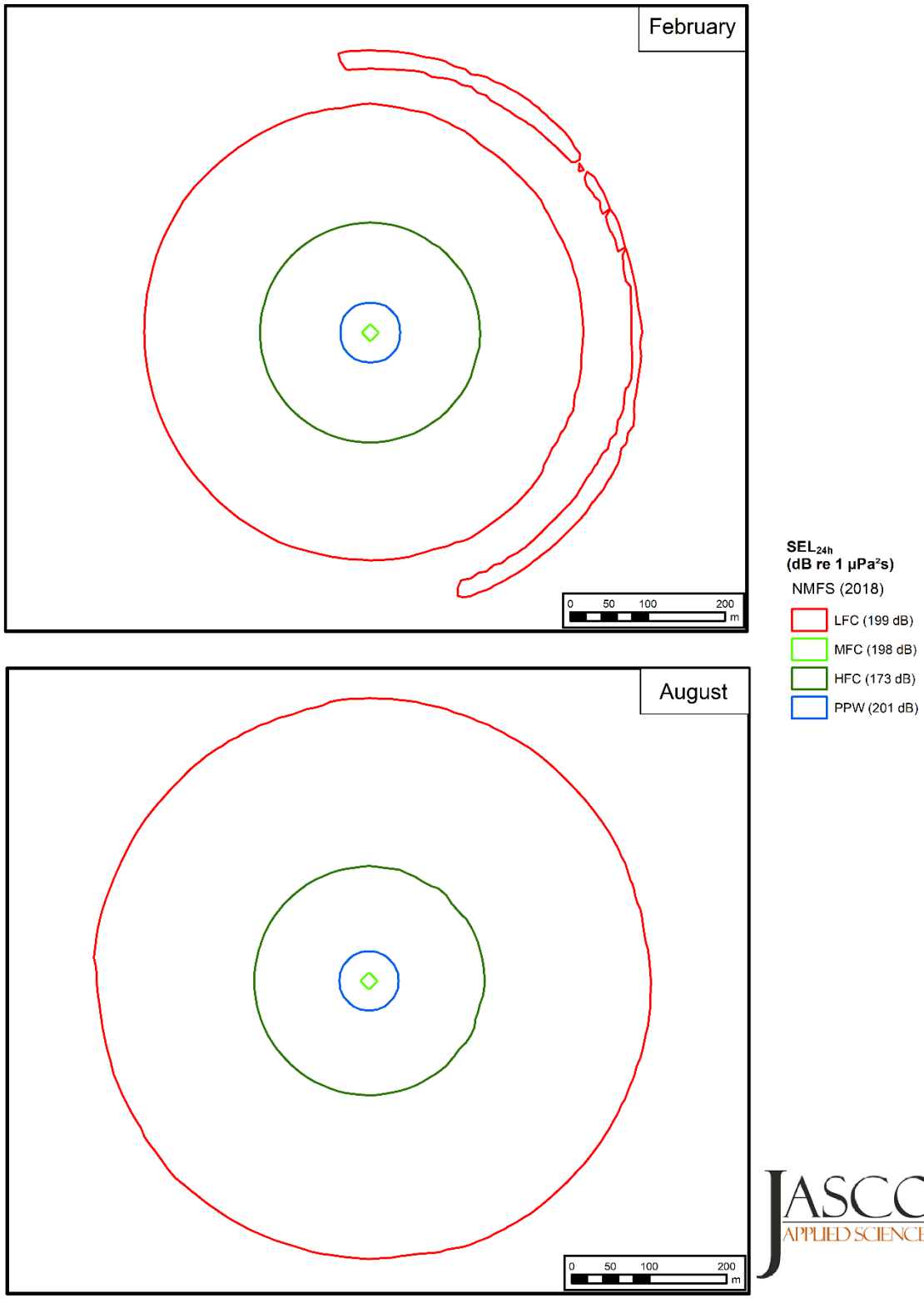

Figure 24. Semisubmersible (*Seadrill West Sirius*): Broadband (10–25,000 Hz) maximum-over-depth M-weighted SEL_{24h} isopleths.

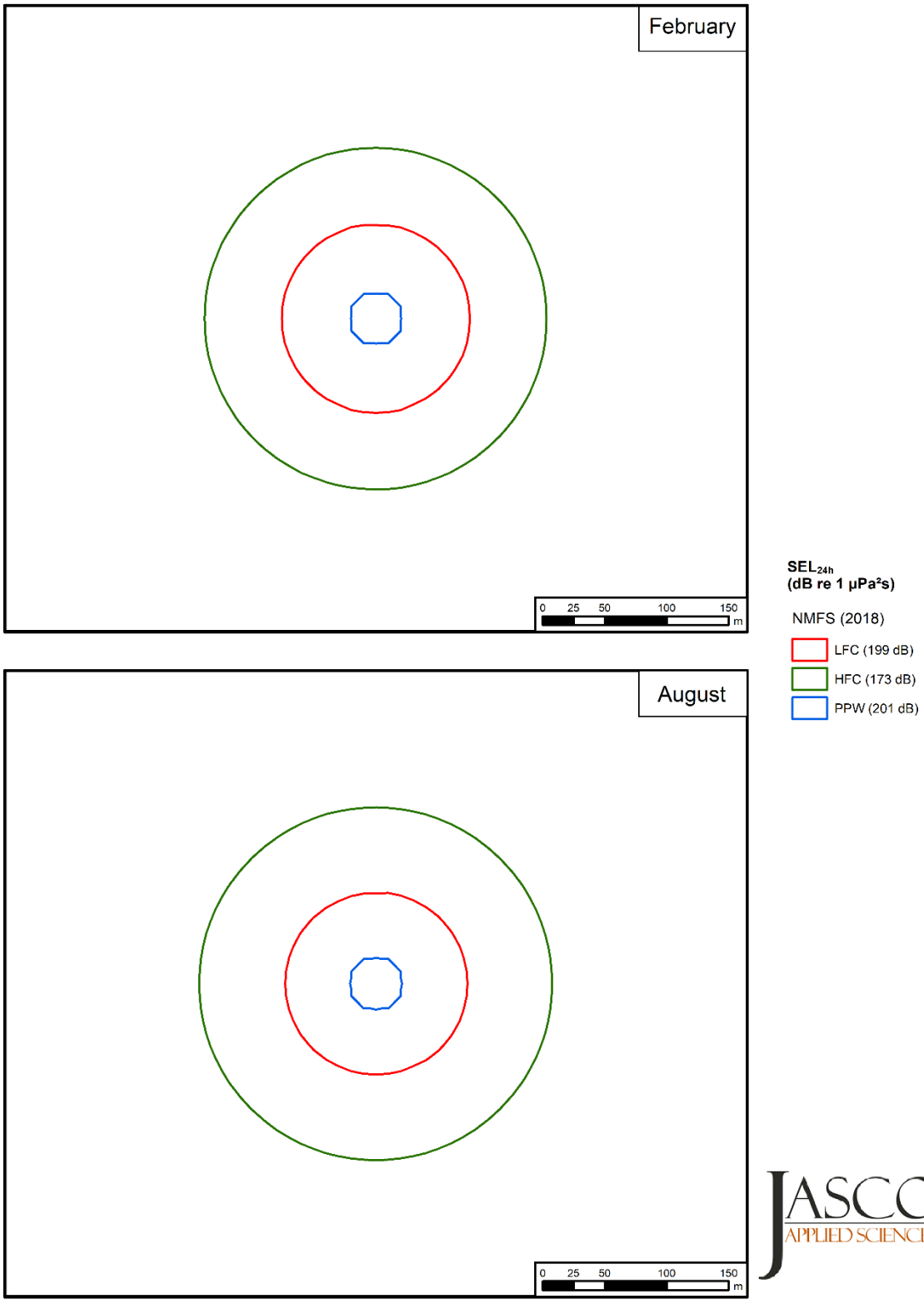

Figure 25. Support Vessel Ops (DVS *Fu Lai*): Broadband (10–25,000 Hz) maximum-over-depth M-weighted SEL_{24h} isopleths.

5. Cumulative Sound Field

A cumulative soundscape study was also performed to consider the total sound field in the project area with sound from the proposed Suncor project added to the sound levels propagating from four other production platforms (Hibernia, Hebron, Terra Nova, and White Rose) and drilling at the Hibernia Southern Extension (HSE)); the modelled activities and broadband source levels are given in Table 14. The modelling results for the cumulative sound are described and compared to the sound levels generated by the Suncor project on its own.

Table 14. Sources that were used for cumulative sound field modelling.

Designation	Activity	Broadband SPL (dB re 1 µPa)		
		Primary activity	Support vessel	Total
Site A – Suncor Project	DP-assist anchored drilling	193.7	178	193.8
S2: Hibernia	Gravity based structure production platform	173.9	178	179.4
S3: Hibernia Southern Ext.	DP-assist anchored drilling	193.7	178	193.8
S4: Hebron	Gravity based structure production platform	173.9	178	179.4
S5: Terra Nova	Floating production storage and offloading	183.7	178	184.7
S6: White Rose	Floating production storage and offloading	183.7	178	184.7

Figure 26 shows the maximum-over-depth broadband 24-hour SEL sound field for the Semisubmersible (*Seadrill West Sirius*) and one support vessel at Site A, along with typical operations (including support vessels) at the five other sites. This can be compared with Figure 27, where the source of sound at Site A has been switched off, but the same sound levels as before kept for the other five sites. It is evident from these figures that the presence or absence of any one of these sound sources has a great impact on the sound field within a maximum radius of about 10 km from the operations site. At further distances, the contribution to the sound field from any one operations site is of lesser significance, compared either to another operations site that is closer, or to the combined sound field of all the operations together.

For example the SEL_{24h} = 180 dB re 1 µPa^2 s contour line extends to a distance about 30 km further in February with the Site A drilling operations active, compared to the same activity at the other sites, but no activity at Site A. For August, the difference in the extent of the same contour line is about 15 km in the two cases. Given that the total radial extent of this contour line is about 90 km in February and 25 km in August, turning off the sound at Site A reduces the extent of this contour line by 30% and 60%, respectively. Different relative effects would be found for other isopleth levels, as this is just one example. The 180 dB re 1 µPa^2 s level for SEL_{24h} is a relatively weak exposure level, well below where injurious marine mammal effects occur.

As can be seen from a comparison of Tables 10–13, as well as Figures 24 and 25, the sound projected (and the biological impact) from the support vessel is clearly less than from the drilling operations itself, but still of a comparable magnitude, and support vessels are part of the other modelled operations as well. Although, for simplicity, we have modelled the support vessels collocated with their associated operations site, in reality they will often be in transit or moving around for other reasons. This would spread-out their 24-hour SEL impact to some extent, and lessen the overall environmental impact.

This analysis applies for typical operations, not when a VSP is in progress. The VSP source is considerably louder than the sounds that are produced in typical operations, and the airgun array will dominate the soundscape when a VSP is in progress.

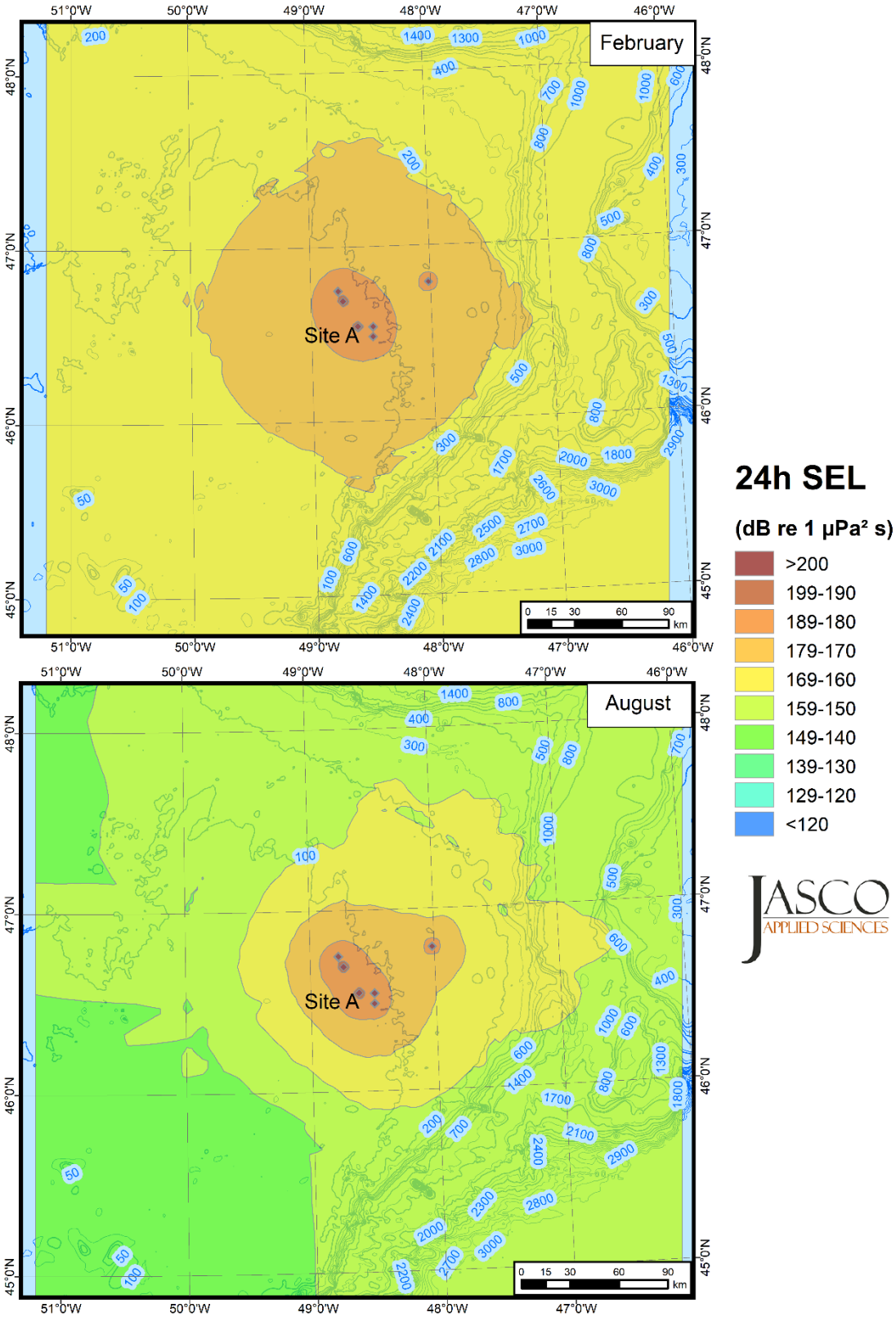

Figure 26. Semisubmersible (*Seadrill West Sirius*) and support vessel at Site A, along with typical operations (including support vessels) at the five other sites. Broadband (10–25,000 Hz) maximum-over-depth 24-hour SEL field.Blue contours indicate water depth in metres.

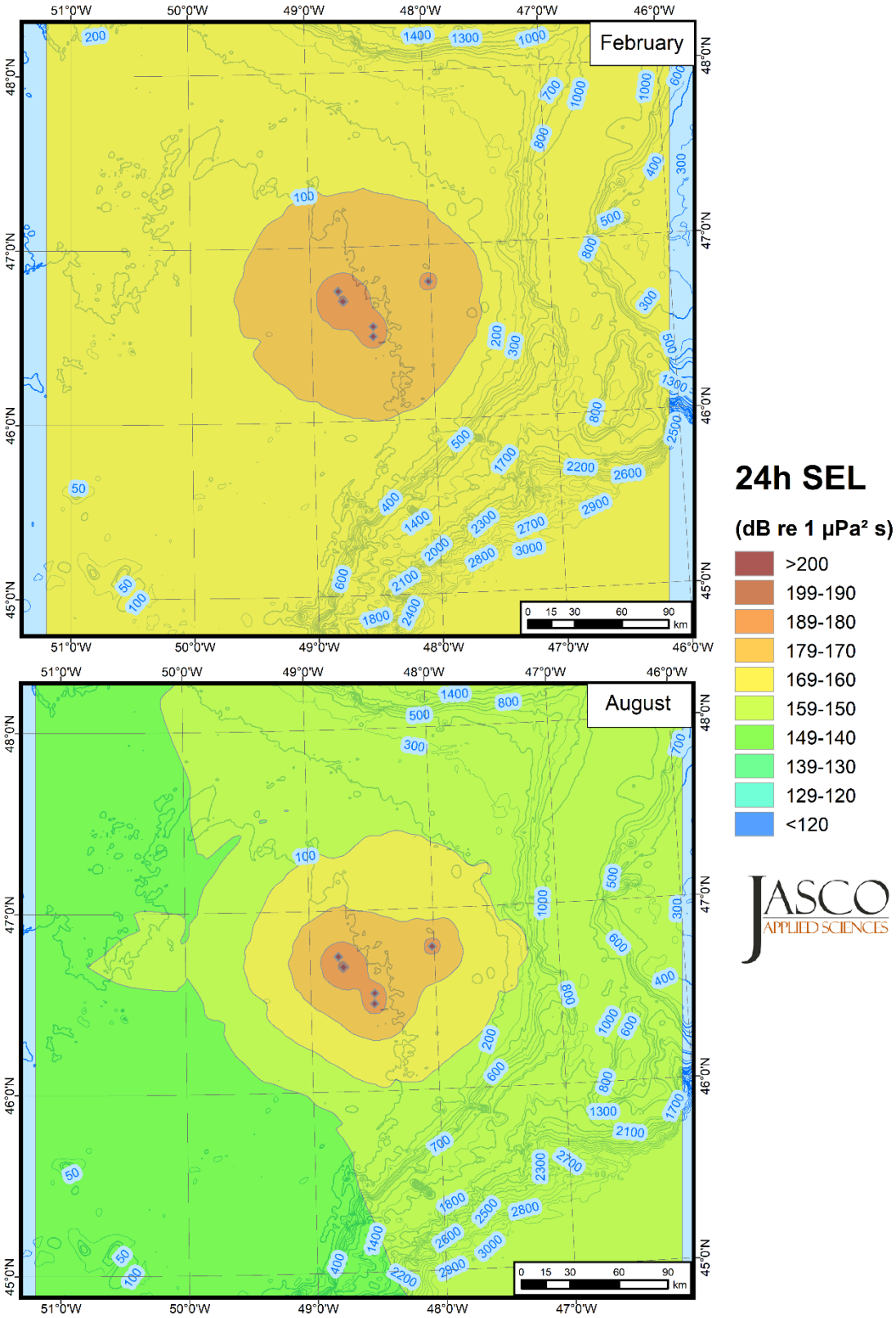

Figure 27. No source at Site A, but with typical operations (including support vessels) at the five other sites. Broadband (10–25,000 Hz) maximum-over-depth 24-hour SEL field. Blue contours indicate water depth in metres.

6. Impacts on Fish

The understanding of the impacts of anthropogenic sound on fish is still evolving, although significant progress has already been made. The following outline from Popper and Hawkins (2019b) provides some background.

> Continuous sounds from activities like shipping increase overall background noise levels, whereas others, including construction work, produce shorter but more intense sounds. Many of these sounds have the potential to affect fish behaviour, whereas the most intense sounds may cause physical harm to animals near the source. In order to regulate sound-producing activities, there is an urgent need to establish sound exposure criteria.
>
> Indeed, a great concern is that anthropogenic sound may be detectable by fishes over great distances, and such sounds can affect fishes in many ways. However, fishes, like humans, may also ignore sounds that are not too loud, some sounds may have no impact upon fishes.
>
> Anthropogenic noise may have a wide range of effects on fishes. Very intense impulsive sounds from explosions, pile driving, and seismic oil and gas surveys may result in death, mortal injuries, adverse effects on hearing abilities and detrimental physiological effects. Continuous sounds, such as those generated by shipping, dredging, trawling, and drilling can change the soundscape dramatically and can interfere with (mask) the detection of natural sounds and cause behavioural changes.
>
> Because of the continued increase in anthropogenic underwater noise from a wide range of sources, there is an urgent need to examine the effects of different types of anthropogenic sounds on fishes under varying conditions of exposure. However, currently there are so many fundamental knowledge gaps on the potential effects of anthropogenic sound on fishes that it is almost impossible to reach clear conclusions on the nature and levels of sound that have potential to cause changes in behaviour or even physical harm.

That being said, there are proposed interim guidelines (Popper and Hawkins 2019a) to limit the impact to fish from anthropogenic activities, such as in this case, exploratory drilling operations and seismic surveys. For the purpose of these guidelines, fish are grouped into five categories (Table 15).

Table 15. Groupings of fish for the purpose of the interim acoustic impact guidelines (Popper and Hawkins 2019a).

Group	Characteristics
1	Fishes lacking swim bladders that are sensitive only to sound particle motion and show sensitivity to only a narrow band of frequencies (*e.g.*, flatfishes, Pleuronectiformes; sharks skates and rays, Chondrichthyes).
2	Fishes with a swim bladder where that organ does not appear to play a role in hearing. These fish are sensitive only to particle motion and show sensitivity to only a narrow band of frequencies. This group includes salmonids (Salmonidae) and some tunas and mackerels (Scombridae), but many other species are likely to fit into this category as well.
3	Fishes with swim bladders that are close, but not intimately connected, to the ear. These fishes are sensitive to both particle motion and sound pressure, and show a more extended frequency range than groups 1 or 2, extending up to about 500 Hz. This group includes cod fishes (Gadidae), eels (Anguillidae), some drums and croakers (Sciaenidae), and perhaps other fishes.
4	Fishes that have special structures mechanically linking the swim bladder to the ear. These fishes are primarily sensitive to sound pressure, although they also detect particle motion. They have a wider frequency range, extending to several kHz and generally show higher sensitivity to sound pressure than fishes in groups 1, 2, or 3. The group includes some of the squirrelfishes (Holocentridae), drums and croakers (Sciaenidae), herrings (Clupeidae) and the large group of otophysan fishes.
5	Eggs and larvae.

The proposed guidelines describe three main types of impact criteria: (a) mortality and potential mortal injury (herein "mortality"), (b) recoverable injury impairment (herein "injury"), and (c) temporary threshold shift impairment (herein "TTS-onset"). There are actually two additional impact types described, of lesser severity (in most cases): masking impairment and behaviour impacts; however, the guidelines for these are unclear in how to apply to the sound fields we are modelling, and we consider those to be out-of-scope for the present study.

Guidelines are proposed for these three impact criteria that involve PK and cumulative SEL. The PK guidelines only apply to impulsive sources (in this case, the VSP). The guidelines do not specify an integration time for accumulating SEL, but for the purpose of this study we will use 24-hour SEL (SEL_{24h}). The numerical limits for these criteria, along with the corresponding threshold radii for the three sources of the present study, are shown in Tables 16–19. The non-mortal thresholds for groups 4 and 5 do not have a numerical criterion; the threat is either high or moderate, as indicated, if the sound is near.

Table 16. Evaluation of the VSP source against the metrics of the proposed interim guidelines for fish acoustic impact criteria for PK (Popper and Hawkins 2019a).

Fish group for acoustic impact guidelines	Mortality					Injury				
	PK (dB re 1 µPa)	February		August		PK (dB re 1 µPa)	February		August	
		R_{max}	$R_{95\%}$	R_{max}	$R_{95\%}$		R_{max}	$R_{95\%}$	R_{max}	$R_{95\%}$
1 – No swim bladder	> 213	0.032	0.032	0.032	0.032	> 213	0.032	0.032	0.032	0.032
2 – Swim bladder not for hearing	> 207	0.067	0.067	0.067	0.067	> 207	0.067	0.067	0.067	0.067
3 – Swim bladder for hearing	> 207	0.067	0.067	0.067	0.067	> 207	0.067	0.067	0.067	0.067
4 – Sea turtles	> 207	0.067	0.067	0.067	0.067	Near-high				
5 – Eggs and larvae	> 207	0.067	0.067	0.067	0.067	Near-moderate				

Table 17. Evaluation of the VSP source against the metrics of the proposed interim guidelines for fish acoustic impact criteria for SEL (Popper and Hawkins 2019a).

Fish group for acoustic impact guidelines	Mortality					Injury					TTS-onset				
	SEL (dB re 1 µPa²·s)	February		August		SEL (dB re 1 µPa²·s)	February		August		SEL (dB re 1 µPa²·s)	February		August	
		R_{max}	$R_{95\%}$	R_{max}	$R_{95\%}$		R_{max}	$R_{95\%}$	R_{max}	$R_{95\%}$		R_{max}	$R_{95\%}$	R_{max}	$R_{95\%}$
1 – No swim bladder	> 219	0.014	0.014	0.014	0.014	> 216	0.022	0.022	0.022	0.022	>> 186	2.78	2.53	2.68	2.32
2 – Swim bladder not for hearing	210	0.041	0.041	0.041	0.041	203	0.220	0.184	0.220	0.180	> 186	2.78	2.53	2.68	2.32
3 – Swim bladder for hearing	207	0.063	0.061	0.063	0.061	203	0.220	0.184	0.220	0.180	186	2.78	2.53	2.68	2.32
4 – Sea turtles	210	0.041	0.041	0.041	0.041	Near-high					Near-high				
5 – Eggs and larvae	> 210	0.041	0.041	0.041	0.041	Near-moderate					Near-moderate				

Table 18. Evaluation of the MODU source against the metrics of the proposed interim guidelines for fish acoustic impact criteria for SEL (Popper and Hawkins 2019a).

Fish group for acoustic impact guidelines	Mortality					Injury					TTS-onset				
	SEL (dB re 1 µPa²·s)	February		August		SEL (dB re 1 µPa²·s)	February		August		SEL (dB re 1 µPa²·s)	February		August	
		R_{max}	$R_{95\%}$	R_{max}	$R_{95\%}$		R_{max}	$R_{95\%}$	R_{max}	$R_{95\%}$		R_{max}	$R_{95\%}$	R_{max}	$R_{95\%}$
1 – No swim bladder	> 219	0.014	0.014	0.014	0.014	> 216	0.032	0.032	0.032	0.032	>> 186	6.04	5.56	6.15	5.60
2 – Swim bladder not for hearing	210	0.073	0.072	0.073	0.072	203	0.264	0.251	0.362	0.345	> 186	6.04	5.56	6.15	5.60
3 – Swim bladder for hearing	207	0.132	0.130	0.134	0.130	203	0.264	0.251	0.362	0.345	186	6.04	5.56	6.15	5.60
4 – Sea turtles	210	0.073	0.072	0.073	0.072	Near-high					Near-high				
5 – Eggs and larvae	> 210	0.073	0.072	0.073	0.072	Near-moderate					Near-moderate				

Table 19. Evaluation of the supply vessel source against the metrics of the proposed interim guidelines for fish acoustic impact criteria for SEL (Popper and Hawkins 2019a).

Fish group for acoustic impact guidelines	Mortality					Injury					TTS-onset				
	SEL (dB re 1 µPa²·s)	February		August		SEL (dB re 1 µPa²·s)	February		August		SEL (dB re 1 µPa²·s)	February		August	
		R_{max}	$R_{95\%}$	R_{max}	$R_{95\%}$		R_{max}	$R_{95\%}$	R_{max}	$R_{95\%}$		R_{max}	$R_{95\%}$	R_{max}	$R_{95\%}$
1 – No swim bladder	> 219	0.014	0.014	0.014	0.014	> 216	0.014	0.014	0.014	0.014	>> 186	2.00	1.76	1.92	1.73
2 – Swim bladder not for hearing	210	0.032	0.032	0.032	0.032	203	0.073	0.072	0.073	0.071	> 186	2.00	1.76	1.92	1.73
3 – Swim bladder for hearing	207	0.045	0.045	0.045	0.042	203	0.073	0.072	0.073	0.071	186	2.00	1.76	1.92	1.73
4 – Sea turtles	210	0.032	0.032	0.032	0.032	Near-high					Near-high				
5 – Eggs and larvae	> 210	0.032	0.032	0.032	0.032	Near-moderate					Near-moderate				

7. Discussion

The acoustic field modelling was performed for two types of sources: a seismic source (impulsive) and thruster-based sources (MODU and vessel, non-impulsive). The propagation conditions were tested for two months (August and February) that feature different sound speed profiles in the water column. The vertical distribution of the acoustic energy is primarily defined by the sound speed profile. The February sound speed profile features a weak surface channel that extends to the bottom (also called a half-channel); although it does allow some long-range acoustic propagation through surface reflections, the water depth is not sufficient for this mechanism to be very effective. The February SSP allows a significant amount of the acoustic energy to reach the bottom, where it is only partly reflected, and partly absorbed. The sound speed profile typical for August features a highly negative velocity gradient in the upper 50 m, which refracts the acoustic waves towards the bottom and acts as a barrier to sound propagation in the upper 50 m. The weakly positive sound speed gradient below 50 m prevents a deep sound channel from forming, so long-range sound propagation is limited in the August SSP.

The propagation of the sound along different azimuths depends on the directivity of the source and the topography of the ocean bottom. The source levels of the 1200 in^3 seismic array in the 100–400 Hz frequency band were higher in the broadside lobe. The source was virtually omnidirectional at frequencies below 100 Hz and above 400 Hz. As a result, the ranges to specific acoustic thresholds were longer for the endfire and broadside directions. The topography defines the spread of the acoustic energy in the vertical dimension. As the water depth increases, the acoustic wave has more space to refract upward without hitting the bottom and losing energy at the bottom interface, as such the transmission loss decreases compared to the profile with constant water depth. For the propagation profiles with decreasing water depth, two effects take place. The decreasing water depth concentrates the acoustic energy within narrower waveguide, which increases the sound levels. Conversely, the acoustic wave interacts with the bottom more often, losing a greater fraction of its energy in the sediment. The latter effect prevails, and propagation profiles with decreasing water depths, such as towards the continental shelf, have higher propagation loss decreases compared to profiles with constant water depths. The bottom topography in the Jeanne d'Arc basin is fairly flat, so this effect is only a minor factor.

The acoustic fields modelled in this study were tested against various impact criteria defined in terms of a single event, per-pulse in case of impulsive sources and per-second for non-impulsive sources, and continuous source operation for a specific time period.

When applying impact criteria based on the SPL signal metric (NMFS 2018) to the sound field from the seismic source (impulsive source type), the ranges from the source to the injury thresholds (in round numbers) were about 82 m and 490 m, for pinnipeds (190 dB) and cetaceans (180 dB), respectively, and 6.50 km to the behavior response threshold (160 dB) for all mammals (Table 6). The PK-based injury criteria were less impactful, in comparison (Table 7). The 24-hour SEL-based criteria were also less impactful for this source (Table 9) for most species, except for low-frequency cetaceans, which had an injury threshold distance of about 2.5 km in February and 2.2 km in August.

The injury thresholds ranges from the semisubmersible (MODU) drilling operations (continuous source type) were more impactful for the 24-hour SEL criteria than the SPL-based criteria, for most species. The SEL_{24} injury threshold for low-frequency cetaceans extended to about 365 m from the MODU and 145 m for high-frequency cetaceans. The SPL injury criteria threshold extended to less than 20 m. The injury threshold ranges to the other animals were less than 40 m (see Table 12). The range to the SPL-based behaviour response threshold from the MODU (120 dB) was about 75 km in February and 38 km in August (Table 10), the SEL-based criteria were only a fraction of this (Table 12).

The ranges to the injury thresholds for the support vessel were well under those for the MODU (typically, between ½ to ¼ of the threshold distance for low-frequency cetaceans and phocid pinnipeds, although more comparable for high-frequency cetaceans). The details can be seen in the previously referenced tables and figures. This is because although the MODU is primarily anchored, the DP-assist uses four of the eight available thrusters; one thruster would be more comparable to a supply vessel. However, the support vessels are modelled as always operating at the same location, which is not atypical, but not necessarily always the case either.

All of these modelling assumptions are precautionary in the sense that, while not exemplifying a worse-case scenario by any means, they are nevertheless assuming somewhat more aggressive sound generation than would probably be the case most of the time.

It should be noted that both SPL and PK signal metrics are calculated based on the unweighted broadband signal, i.e., the hearing frequency band of specific marine mammals is not taken into account, and M-weighting functions are not applied in this case, like they are for the SEL-based criteria.

For the modelled impacts on fish, Section 6 has employed the proposed interim impact criteria of (Popper and Hawkins 2019a). Based on these criteria, fish mortality would be confined to a distance of 67 m from the VSP source (a result of the PK threshold, Table 16; the SEL threshold for a 24-hour accumulation period resulted in similar, but slightly shorter injury ranges, Table 17). For the MODU, the zone of mortality to a distance of up to 135 m for some species (Table 18). For the supply vessel, this distance is 45 m (Table 19). There is very little seasonal dependence in the fish mortality threshold distances, due to the short propagation ranges involved.

Literature Cited

[ISO] International Organization for Standardization. 2017. *ISO 18405:2017. Underwater acoustics – Terminology*. Geneva. https://www.iso.org/standard/62406.html.

[NMFS] National Marine Fisheries Service (US). 2016. *Technical Guidance for Assessing the Effects of Anthropogenic Sound on Marine Mammal Hearing: Underwater Acoustic Thresholds for Onset of Permanent and Temporary Threshold Shifts*. US Department of Commerce, NOAA. NOAA Technical Memorandum NMFS-OPR-55. p. 178.

[NMFS] National Marine Fisheries Service (US). 2018. *2018 Revision to: Technical Guidance for Assessing the Effects of Anthropogenic Sound on Marine Mammal Hearing (Version 2.0): Underwater Thresholds for Onset of Permanent and Temporary Threshold Shifts*. US Department of Commerce, NOAA. NOAA Technical Memorandum NMFS-OPR-59. p. 167. https://www.fisheries.noaa.gov/webdam/download/75962998.

Abid, I.A., R. Hesse, and J.D. Harper. 2004. Variation in mixed-layer illite/smectite diagenesis in the rift and post-rift sediments of the Jeanne D'Arc Basin, Grand Banks, offshore Newfoundland, Canada. *Can. J. Earth Sci.* 41: 401–429.

Aerts, L.A.M., M. Blees, S.B. Blackwell, C.R. Greene, Jr., K.H. Kim, D.E. Hannay, and M.E. Austin. 2008. Marine mammal monitoring and mitigation during BP Liberty OBC seismic survey in Foggy Island Bay, Beaufort Sea, July-August 2008: 90-day report. Document P1011-1. Report by LGL Alaska Research Associates Inc., LGL Ltd., Greeneridge Sciences Inc., and JASCO Applied Sciences for BP Exploration Alaska. p. 199. ftp://ftp.library.noaa.gov/noaa_documents.lib/NMFS/Auke%20Bay/AukeBayScans/Removable%20Disk/P1011-1.pdf.

ANSI S1.1-2013. 2013. *American National Standard Acoustical Terminology*. American National Standards Institute, NY, USA.

Austin, M.E. and Z. Li. 2016. Marine Mammal Monitoring and Mitigation During Exploratory Drilling by Shell in the Alaskan Chukchi Sea, July–October 2015: Draft 90-day report. In: Ireland, D.S. and L.N. Bisson (eds.). Underwater Sound Measurements. LGL Rep. P1363D. Report from LGL Alaska Research Associates Inc., LGL Ltd., and JASCO Applied Sciences Ltd. For Shell Gulf of Mexico Inc, National Marine Fisheries Service, and US Fish and Wildlife Service. 188 pp + appendices.

Austin, M.E., D.E. Hannay, and K.C. Bröker. 2018. Acoustic characterization of exploration drilling in the Chukchi and Beaufort seas. *The Journal of the Acoustical Society of America* 144(1): 115-123. https://asa.scitation.org/doi/abs/10.1121/1.5044417.

Becker, J.J., D.T. Sandwell, W.H.F. Smith, J. Braud, B. Binder, J. Depner, D. Fabre, J. Factor, S. Ingalls, et al. 2009. Global Bathymetry and Elevation Data at 30 Arc Seconds Resolution: SRTM30_PLUS. *Marine Geodesy* 32(4): 355-371. https://doi.org/10.1080/01490410903297766.

Brown, N.A. 1977. Cavitation noise problems and solutions. *International Symposium on Shipboard Acoustics*. 6-10 Sep 1976, Noordwijkehout. p. 17.

Carnes, M.R. 2009. Description and Evaluation of GDEM-V 3.0. US Naval Research Laboratory, Stennis Space Center, MS. NRL Memorandum Report 7330-09-9165. p. 21. https://apps.dtic.mil/dtic/tr/fulltext/u2/a494306.pdf.

Černý, V. 1985. Thermodynamical approach to the traveling salesman problem: An efficient simulation algorithm. *Journal of Optimization Theory and Applications* 45(1): 41-51. https://doi.org/10.1007/BF00940812.

Collins, M.D. 1993. A split-step Padé solution for the parabolic equation method. *Journal of the Acoustical Society of America* 93(4): 1736-1742. https://doi.org/10.1121/1.406739.

Collins, M.D., R.J. Cederberg, D.B. King, and S. Chin-Bing. 1996. Comparison of algorithms for solving parabolic wave equations. *Journal of the Acoustical Society of America* 100(1): 178-182. https://doi.org/10.1121/1.415921.

Coppens, A.B. 1981. Simple equations for the speed of sound in Neptunian waters. *Journal of the Acoustical Society of America* 69(3): 862-863. https://doi.org/10.1121/1.382038.

Divins, D.L. 2010. *NGDC Total Sediment Thickness of the World's Oceans & Marginal Seas* (webpage). ArcGIS files. http://www.ngdc.noaa.gov/mgg/sedthick/sedthick.html.

Dragoset, W.H. 1984. A comprehensive method for evaluating the design of airguns and airgun arrays. *16th Annual Offshore Technology Conference* Volume 3, 7-9 May 1984. OTC 4747, Houston, TX, USA. pp 75–84.

Ellis, D. and S. Hughes. 1989. Estimates of sediment properties for ARPS. Dartmouth, Nova Scotia, Canada, 12 July 1989.

Finneran, J.J. 2015. Auditory weighting functions and TTS/PTS exposure functions for cetaceans and marine carnivores. Technical report by SSC Pacific, San Diego, CA, USA.

Finneran, J.J. 2016. Auditory weighting functions and TTS/PTS exposure functions for marine mammals exposed to underwater noise. Technical Report for Space and Naval Warfare Systems Center Pacific, San Diego, CA, USA. p. 49. http://www.dtic.mil/dtic/tr/fulltext/u2/1026445.pdf.

Fisher, F.H. and V.P. Simmons. 1977. Sound absorption in sea water. *Journal of the Acoustical Society of America* 62(3): 558-564. https://doi.org/10.1121/1.381574.

Funk, D., D.E. Hannay, D.S. Ireland, R. Rodrigues, and W.R. Koski (eds.). 2008. *Marine mammal monitoring and mitigation during open water seismic exploration by Shell Offshore Inc. in the Chukchi and Beaufort Seas, July–November 2007: 90-day report*. LGL Report P969-1. Prepared by LGL Alaska Research Associates Inc., LGL Ltd., and JASCO Research Ltd. for Shell Offshore Inc., National Marine Fisheries Service (US), and US Fish and Wildlife Service. 218 p.

Hannay, D.E. and R.G. Racca. 2005. Acoustic Model Validation. Document 0000-S-90-04-T-7006-00-E, Revision 02. Technical report by JASCO Research Ltd. for Sakhalin Energy Investment Company Ltd. p. 34.

Harrison, C.H. and J.A. Harrison. 1995. A simple relationship between frequency and range averages for broadband sonar. *Journal of the Acoustical Society of America* 97(2): 1314-1317. https://doi.org/10.1121/1.412172.

Ireland, D.S., R. Rodrigues, D. Funk, W.R. Koski, and D.E. Hannay. 2009. Marine mammal monitoring and mitigation during open water seismic exploration by Shell Offshore Inc. in the Chukchi and Beaufort Seas, July–October 2008: 90-Day Report. Document P1049-1. p. 277.

King, E.L. and G.V. Sonnichsen. 2000. New insight into glaciations and sea-level fluctuation on the northern Grand Banks, offshore Newfoundland. Geological Survey of Canada, Current Research 2000-D6. p. 10.

Landro, M. 1992. Modeling of GI gun signatures. *Geophysical Prospecting* 40: 721–747. https://doi.org/10.1111/j.1365-2478.1992.tb00549.x

Laws, R.M., L. Hatton, and M. Haartsen. 1990. Computer modeling of clustered airguns. *First Break* 8(9): 331–338.

Leggat, L.J., H.M. Merklinger, and J.L. Kennedy. 1981. LNG Carrier Underwater Noise Study for Baffin Bay. Defence Research Establishment Atlantic, Dartmouth, NS, Canada. p. 32.

Lurton, X. 2002. *An Introduction to Underwater Acoustics: Principles and Applications*. Springer, Chichester, UK. 347 p.

MacGillivray, A.O. 2006. Underwater Acoustic Source Level Measurements of Castoro Otto and Fu Lai. Technical report by JASCO Research.

MacGillivray, A.O. and N.R. Chapman. 2012. Modeling underwater sound propagation from an airgun array using the parabolic equation method. *Canadian Acoustics* 40(1): 19-25. https://jcaa.caa-aca.ca/index.php/jcaa/article/view/2502/2251.

Mattsson, A. and M. Jenkerson. 2008. Single Airgun and Cluster Measurement Project. *Joint Industry Programme (JIP) on Exploration and Production Sound and Marine Life Proramme Review*. 28-30 Oct. International Association of Oil and Gas Producers, Houston, TX, USA.

Mosher, D.C. and G.V. Sonnichsen. 1992. Stratigraphy and Sedimentology of sediments on the northeastern Grand Banks of Newfoundland from borehole investigation. Geophysical Journal of the Royal Astronomical Society. Geological Survey of Canada, Open File 2409. p. 110.

O'Neill, C., D. Leary, and A. McCrodan. 2010. Sound Source Verification. (Chapter 3) *In* Blees, M.K., K.G. Hartin, D.S. Ireland, and D.E. Hannay (eds.). *Marine mammal monitoring and mitigation during open water seismic exploration by Statoil USA E&P Inc. in the Chukchi Sea, August-October 2010: 90-day report*. LGL Report P1119. Prepared by LGL Alaska Research Associates Inc., LGL Ltd., and JASCO Applied Sciences Ltd. for Statoil USA E&P Inc., National Marine Fisheries Service (US), and US Fish and Wildlife Service. pp 1-34.

Osler, J. 1994. A geo-acoustic and oceanographic description of several shallow water experimental sites on the Scotian Shelf. Technical Memorandum Report 94/216. DREA, Dartmouth, Nova Scotia, Canada. p. pp. 47.

Popper, A.N. and A.D. Hawkins. 2019a. An overview of fish bioacoustics and the impacts of anthropogenic sounds on fishes (Review Paper). *Journal of Fish Biology*: 1-22. https://doi.org/10.1111/jfb.13948.

Popper, A.N. and A.D. Hawkins. 2019b. Impacts of Anthropogenic Noise on Fishes. Fisheries Society of the British Isles (FSBI) Briefing Paper. p. 4. https://www.fsbi.org.uk/wp-content/uploads/2019/04/FSBI%20Briefing%20Note%20Impacts%20of%20Anthropogenic%20Noise%20on%20Fishes.pdf.

Popper, A.N., A.D. Hawkins, and M.B. Halvorsen. 2019. Anthropogenic Sound and Fishes. Report WA-RD 891.1. Report by ICF for Washington State Department of Transportation, Research Office. p. 170.

Porter, M.B. and Y.-C. Liu. 1994. Finite-element ray tracing. *In*: Lee, D. and M.H. Schultz (eds.). *International Conference on Theoretical and Computational Acoustics*. Volume 2. World Scientific Publishing Co. pp 947-956.

Racca, R.G. and J.A. Scrimger. 1986. Underwater Acoustic Source Characteristics of Air and Water Guns. Report 06SB 97708-5-7055. Report by JASCO Research Ltd. for Defence Research Establishment Pacific (Canada), Victoria, BC, Canada.

Ross, D. 1976. *Mechanics of Underwater Noise*. Pergamon Press, NY, USA.

Siderius, M. and M.B. Porter. 2006. Modeling techniques for marine-mammal risk assessment. *IEEE Journal of Oceanic Engineering* 31(1): 49-60. https://doi.org/10.1109/JOE.2006.872211.

Smith, W.H.F. and D.T. Sandwell. 1997. Global sea floor topography from satellite altimetry and ship depth soundings. *Science* 277(5334): 1956-1962. https://science.sciencemag.org/content/277/5334/1956.

Southall, B.L., A.E. Bowles, W.T. Ellison, J.J. Finneran, R.L. Gentry, C.R. Greene, Jr., D. Kastak, D.R. Ketten, J.H. Miller, et al. 2007. Marine Mammal Noise Exposure Criteria: Initial Scientific Recommendations. *Aquatic Mammals* 33(4): 411-521.

Spence, J.H., R. Fischer, M.A. Bahtiarian, L. Boroditsky, N. Jones, and R. Dempsey. 2007. Review of Existing and Future Potential Treatments for Reducing Underwater Sound from Oil and Gas Industry Activities. Report NCE 07-001. Report by Noise Control Engineering, Inc. for the Joint Industry Programme on E&P Sound and Marine Life. p. 185.

Teague, W.J., M.J. Carron, and P.J. Hogan. 1990. A comparison between the Generalized Digital Environmental Model and Levitus climatologies. *Journal of Geophysical Research* 95(C5): 7167-7183. https://doi.org/10.1029/JC095iC05p07167.

Warner, G.A., C. Erbe, and D.E. Hannay. 2010. Underwater Sound Measurements. (Chapter 3) *In* Reiser, C.M., D. Funk, R. Rodrigues, and D.E. Hannay (eds.). *Marine Mammal Monitoring and Mitigation during Open Water Shallow Hazards and Site Clearance Surveys by Shell Offshore Inc. in the Alaskan Chukchi Sea, July-October 2009: 90-Day Report*. LGL Report P1112-1. Report by LGL Alaska Research Associates Inc. and JASCO Applied Sciences for Shell Offshore Inc., National Marine Fisheries Service (US), and Fish and Wildlife Service (US). pp 1-54.

Zhang, Z.Y. and C.T. Tindle. 1995. Improved equivalent fluid approximations for a low shear speed ocean bottom. *Journal of the Acoustical Society of America* 98(6): 3391-3396. https://doi.org/10.1121/1.413789.

Ziolkowski, A. 1970. A method for calculating the output pressure waveform from an air gun. *Geophysical Journal of the Royal Astronomical Society* 21(2): 137-161. https://doi.org/10.1111/j.1365-246X.1970.tb01773.x.

Appendix A. Acoustic Metrics

Underwater sound pressure amplitude is measured in decibels (dB) relative to a fixed reference pressure of p_0 = 1 µPa. Because the perceived loudness of sound, especially pulsed noise such as from seismic airguns, pile driving, and sonar, is not generally proportional to the instantaneous acoustic pressure, several sound level metrics are commonly used to evaluate noise and its effects on marine life. Here we provide specific definitions of relevant metrics used in the accompanying report. Where possible, we follow the American National Standard Institute and International Organization for Standardization definitions and symbols for sound metrics (e.g., ANSI 2013, ISO 2017), but these standards are not always consistent.

The zero-to-peak sound pressure, or peak sound pressure (PK or $L_{p,pk}$; dB re 1 µPa), is the decibel level of the maximum instantaneous acoustic pressure in a stated frequency band attained by an acoustic pressure signal, $p(t)$:

$$L_{\mathrm{p,pk}} = 10\log_{10}\frac{\max|p^2(t)|}{p_0^2} = 20\log_{10}\frac{\max|p(t)|}{p_0} \tag{A-1}$$

PK is often included as a criterion for assessing whether a sound is potentially injurious; however, because it does not account for the duration of a noise event, it is generally a poor indicator of perceived loudness.

The sound pressure level (SPL or L_p; dB re 1 µPa) is the root-mean-square (rms) pressure level in a stated frequency band over a specified time window (T; s). It is important to note that SPL always refers to an rms pressure level and therefore not instantaneous pressure:

$$L_{\mathrm{p}} = 10\log_{10}\left(\frac{1}{T}\int_T g(t)\,p^2(t)\,dt \Big/ p_0^2\right) \tag{A-2}$$

where $g(t)$ is an optional time weighting function. In many cases, the start time of the integration is marched forward in small time steps to produce a time-varying SPL function. For short acoustic events, such as sonar pulses and marine mammal vocalizations, it is important to choose an appropriate time window that matches the duration of the signal. For in-air studies, when evaluating the perceived loudness of sounds with rapid amplitude variations in time, the time weighting function $g(t)$ is often set to a decaying exponential function that emphasizes more recent pressure signals. This function mimics the leaky integration nature of mammalian hearing. For example, human-based fast time-weighted SPL ($L_{p,fast}$) applies an exponential function with time constant 125 ms. A related simpler approach used in underwater acoustics sets $g(t)$ to a boxcar (unity amplitude) function of width 125 ms; the results can be referred to as $L_{p,boxcar\ 125ms}$.

The sound exposure level (SEL or L_E; dB re 1 µPa²·s) is the time-integral of the squared acoustic pressure over a duration (T):

$$L_{\mathrm{E}} = 10\log_{10}\left(\int_T p^2(t)\,dt \Big/ T_0 p_0^2\right) \tag{A-3}$$

where T_0 is a reference time interval of 1 s. SEL continues to increase with time when non-zero pressure signals are present. It is a dose-type measurement, so the integration time applied must be carefully considered in terms of relevance for impact to the exposed recipients.

SEL can be calculated over a fixed duration, such as the time of a single event or a period with multiple acoustic events. When applied to pulsed sounds, SEL can be calculated by summing the SEL of the N individual pulses. For a fixed duration, the square pressure is integrated over the duration of interest. For multiple events, the SEL can be computed by summing (in linear units) the SEL of the N individual events:

$$L_{\mathrm{E,N}} = 10 \log_{10} \sum_{i=1}^{N} 10^{\frac{L_{E,i}}{10}} \tag{A-4}$$

Appendix B. Marine Mammal Impact Criteria

B.1. Sound Pressure Level (SPL)

The National Marine Fisheries Service (NMFS) SPL criteria for injury to marine mammals from acoustic exposure were set according to recommendations for cautionary estimates of sound levels leading to onset of permanent hearing threshold shift (PTS). These criteria prescribed injury thresholds of 190 dB re 1 µPa SPL for pinnipeds and 180 dB re 1 µPa SPL for cetaceans, for all types of sound sources except tactical sonar and explosives (NMFS 2018). These injury thresholds are applied to individual noise pulses or instantaneous sound levels and do not consider the overall duration of the noise or its acoustic frequency distribution.

Criteria that do not account for exposure duration or noise spectra are generally insufficient on their own for assessing hearing injury.

B.2. Sound Exposure Level (SEL) and Peak SPL (PK)

In recognition of shortcomings of the SPL-only based injury criteria, in 2005 NMFS sponsored the Noise Criteria Group to review literature on marine mammal hearing to propose new noise exposure criteria. Members of this expert group published a landmark paper (Southall et al. 2007) that suggested assessment methods similar to those applied for humans. The resulting recommendations introduced dual acoustic injury criteria for impulsive sounds that included peak pressure level thresholds and SEL_{24h} thresholds, where the subscripted 24 h refers to the accumulation period for calculating SEL.

SEL_{24h} is frequency weighted according to one of five marine mammal species hearing groups: low-, mid- and high-frequency cetaceans (LFC, MFC, and HFC respectively) and phocids, earless or true seals (pinnipeds), and otariids, eared seals (PPW and OPW, respectively). The onset threshold levels for Temporary Threshold Shift (TTS) and Permanent Threshold Shift (PTS) differ by group and are applied to M-weighted SEL.

B.2.1. Marine Mammal Auditory Weighting Functions (NMFS 2018)

In 2015, a U.S. Navy technical report by Finneran (2015) recommended new auditory weighting functions. The overall shape of the auditory weighting functions is similar to human A-weighting functions, which follows the sensitivity of the human ear at low sound levels. The new frequency-weighting function is expressed as:

$$G(f) = K + 10\log_{10}\left[\left(\frac{(f/f_{lo})^{2a}}{\left[1+(f/f_{lo})^{2}\right]^{a}\left[1+(f/f_{hi})^{2}\right]^{b}}\right)\right], \quad \text{(B-1)Finneran (2015)}$$

proposed five functional hearing groups for marine mammals in water: low-, mid-, and high-frequency cetaceans, phocid pinnipeds, and otariid pinnipeds. The parameters for these frequency-weighting functions were further modified the following year (Finneran 2016) and were adopted in NOAA's technical guidance that assesses noise impacts on marine mammals (NMFS 2016), which was updated two years later after extensive consultations within the scientific community (NMFS 2018). The updates did not affect the content related to either the m-weighting functions definitions or the threshold values. Table B-1 lists the frequency-weighting parameters for each hearing group; Figure B-1 shows the resulting frequency-weighting curves.

Table B-1. Parameters for the auditory weighting functions recommended by NMFS (2018).

Hearing group	*a*	*b*	f_{lo} (Hz)	f_{hi} (Hz)	*K* (dB)
Low-frequency cetaceans	1.0	2	200	19,000	0.13
Mid-frequency cetaceans	1.6	2	8,800	110,000	1.20
High-frequency cetaceans	1.8	2	12,000	140,000	1.36
Phocid pinnipeds in water	1.0	2	1,900	30,000	0.75
Otariid pinnipeds in water	2.0	2	940	25,000	0.64

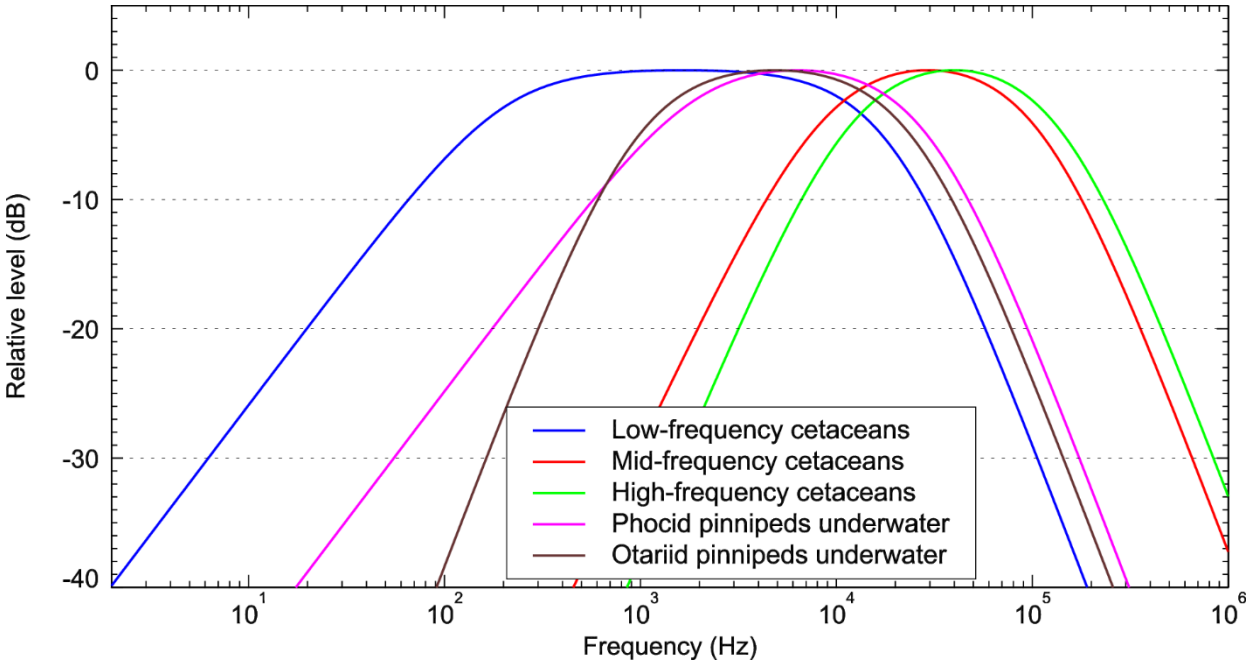

Figure B-1. Auditory weighting functions for functional marine mammal hearing groups as recommended by NMFS (2018).

B.2.2. Impact Thresholds (NMFS 2018)

The PTS- and TTS-onset threshold levels for each hearing group (NMFS 2018) are listed in Table B-2. The threshold levels are defined separately for impulsive sources (e.g., seismic airgun arrays, echosounders) and non-impulsive sources (e.g., vessels). The SEL thresholds are applicable to weighted acoustic fields, while the PK fields are tested against the thresholds without application of the weighting functions.

Table B-2. TTS- and PTS-onset levels for defined marine mammal groups by NMFS (2018).

Hearing group	Non-impulsive		Impulsive			
	SEL (weighted) (dB re 1 µPa²·s)		SEL (weighted) (dB re 1 µPa²·s)		peak SPL (non-weighted) (dB re 1 µPa)	
	TTS-onset	PTS-onset	TTS-onset	PTS-onset	TTS-onset	PTS-onset
Low-frequency cetaceans (LFC)	179	199	168	183	213	219
Mid-frequency cetaceans (MFC)	178	198	170	185	224	230
High-frequency cetaceans (HFC)	153	173	140	155	196	202
Phocid pinnipeds underwater (PPW)	181	201	170	185	212	218
Otariid pinnipeds in water (OPW)	199	219	188	203	226	232

B.2.3. Impact Thresholds (NMFS 2018)

The M-weighting functions have unity gain (0 dB) through the passband and their high and low frequency roll-offs are approximately –12 dB per octave. The amplitude response in the frequency domain of each M-weighting function is defined by:

$$G(f) = -20\log_{10}\left[\left(1+\frac{a^2}{f^2}\right)\left(1+\frac{f^2}{b^2}\right)\right] \quad (14)$$

where G(f) is the weighting function amplitude (in dB) at the frequency f (in Hz), and a and b are the estimated lower and upper hearing limits, respectively, which control the roll-off and passband of the weighting function. The parameters a and b are defined uniquely for each functional hearing group (Table 20).

The auditory weighting functions recommended by Southall et al. (2007) are shown in Figure 28.

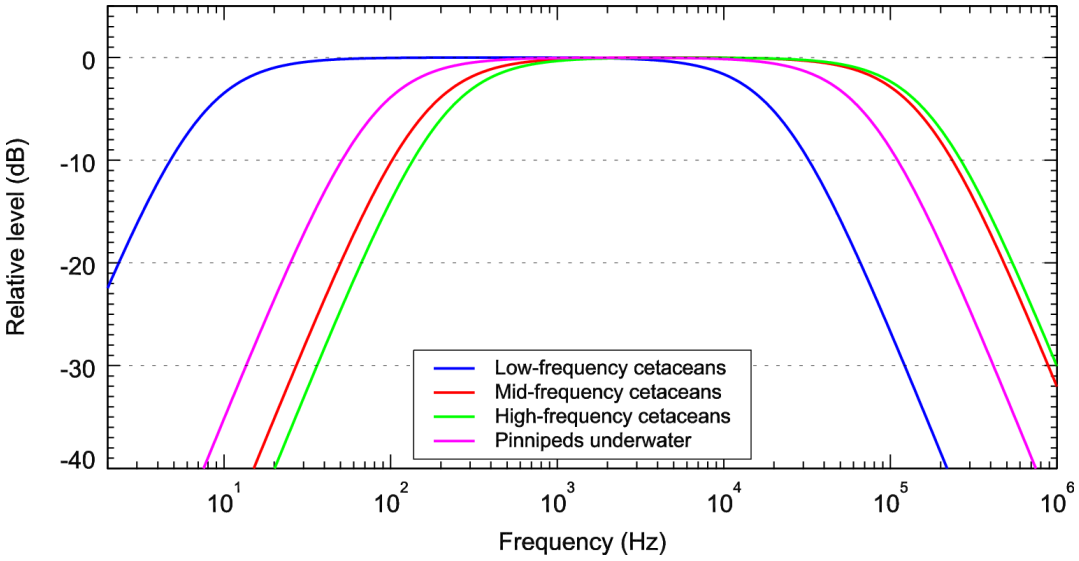

Figure 28. Auditory weighting functions for functional marine mammal hearing groups as recommended by Southall et al. (2007).

Table 20. Parameters for the auditory weighting functions recommended by Southall et al. (2007).

Functional hearing group	a (Hz)	b (Hz)
Low-frequency cetaceans	7	22,000
Mid-frequency cetaceans	150	160,000
High-frequency cetaceans	200	180,000
Pinnipeds in water	75	75,000

Southall et al. (2007) introduced dual injury criteria consisting of both zero-to-peak (peak) SPL thresholds, expressed in dB re 1 µPa, and cumulative SEL thresholds, expressed in dB re 1 µPa^2·s (Table 21). A PTS-onset (injury) is assumed to occur if a received sound exposure exceeds the PK criterion, the SEL criterion, or both. The PK is not frequency weighted whereas the SEL is frequency-weighted using m-weighting function related to the specific marine mammal functional hearing group.

Table 21. PK (dB re 1 µPa) and auditory-weighted cumulative SEL (dB re 1 µPa^2·s) dual acoustic thresholds for permanent threshold shift (PTS) from impulsive and non-impulsive sounds proposed by Southall et al. (2007).

Functional hearing group	Impulsive sound		Non-impulsive sound	
	Peak SPL	Weighted SEL	Peak SPL	Weighted SEL
Low-frequency cetaceans	230	198	230	215
Mid- frequency cetaceans	230	198	230	215
High-frequency cetaceans	230	198	230	215
Pinnipeds in water	218	186	218	203

The PTS-onset thresholds based on PK metric were estimated by adding 6 dB to the known or assumed PK of elicit TTS-onset. The PTS-onset thresholds based on cumulative SEL metric were estimated by

adding 15 dB (for impulsive sounds) and 20 dB (for non-impulsive sounds) to the known or assumed cumulative SEL of elicit TTS-onset.

Unlike NMFS criteria, Southall et al. (2007) criteria consider not only the factor of individual pulses impact, but also a temporal factor, i.e., the history of the exposure to the sound over a specific period of time. For the impulsive sound the shape of the pulse was not considered any more, only the maximum amplitude.